

# ART: Distribution-Free and Model-Agnostic Changepoint Detection with Finite-Sample Guarantees

Xiaolong Cui, Haoyu Geng, Guanghui Wang, Zhaojun Wang and Changliang Zou

*School of Statistics and Data Science, Nankai University, China*

## Abstract

We introduce ART, a distribution-free and model-agnostic framework for changepoint detection that provides finite-sample guarantees. ART transforms independent observations into real-valued scores via a symmetric function, ensuring exchangeability in the absence of changepoints. These scores are then ranked and aggregated to detect distributional changes. The resulting test offers exact Type-I error control, agnostic to specific distributional or model assumptions. Moreover, ART seamlessly extends to multi-scale settings, enabling robust multiple changepoint estimation and post-detection inference with finite-sample error rate control. By locally ranking the scores and performing aggregations across multiple prespecified intervals, ART identifies changepoint intervals and refines subsequent inference while maintaining its distribution-free and model-agnostic nature. This adaptability makes ART as a reliable and versatile tool for modern changepoint analysis, particularly in high-dimensional data contexts and applications leveraging machine learning methods.

**Keywords:** Changepoint detection; Distribution-free inference; Finite-sample guarantees; Model-agnostic methods; Rank-based statistics

## 1 Introduction

Changepoint analysis focuses on identifying abrupt changes in data sequences, a common occurrence when an underlying process evolves over time or across other indexing domains.

Such changes arise in diverse settings, including mean-level shifts in financial series, disruptions in genomic profiles, and anomalies in streaming sensor data.

Over the past few decades, extensive research has examined whether, and where, one or more changepoints occur. Early efforts explored specific finite-dimensional parametric models (Csörgö and Horváth, 1997; Killick et al., 2012; Truong et al., 2020) and nonparametric models (Matteson and James, 2014; Zou et al., 2014; Lung-Yut-Fong et al., 2015; Chen and Zhang, 2015; Arlot et al., 2019). More recent studies address high-dimensional scenarios, investigating changes in means (Bai, 2010; Jirak, 2015; Cho and Fryzlewicz, 2015; Wang and Samworth, 2018; Wang et al., 2018; Liu et al., 2020; Yu and Chen, 2021; Zhang et al., 2022; Wang and Feng, 2023), regression coefficients (Lee et al., 2016; Leonardi and Bühlmann, 2016; Kaul et al., 2019; Wang et al., 2021; Xu et al., 2024), and general distributional shifts (Londschien et al., 2023; Li et al., 2024). Concurrently, a growing literature emphasizes uncertainty quantification of detected changepoints (Hao et al., 2013; Frick et al., 2014; Fang et al., 2020; Chen et al., 2023; Fryzlewicz, 2024a,b) and post-detection inference (Hyun et al., 2018, 2021; Duy et al., 2020; Jewell et al., 2022; Carrington and Fearnhead, 2025). These developments are crucial, given that perfect model recovery is often elusive in practice.

Most changepoint testing procedures rely on asymptotic null distributions to obtain critical values. These tests often guide changepoint estimation methods such as binary segmentation (Fryzlewicz, 2014; Baranowski et al., 2019; Kovács et al., 2023; Yu and Chen, 2021), moving windows (Niu and Zhang, 2012; Eichinger and Kirch, 2018), and scanning-based algorithms (Chan and Walther, 2013). In addition, the critical values or corresponding p-values help control global error rates for uncertainty quantification (Frick et al., 2014; Fang et al., 2020; Fryzlewicz, 2024a). However, convergence to asymptotic null distributions can often be slow (Csörgö and Horváth, 1997), and their accuracies usually depend on stringent assumptions about the data distribution and model form. These approximations become even more fragile in high-dimensional or complex changepoint settings, especially when flexible estimation procedures are employed (Zhao et al., 2024; Londschien et al., 2023). Collectively, these limitations can erode the reliability of changepoint testing, estimation, and post-detection inference in finite-sample scenarios.

To reduce reliance on specific parametric models and distributional assumptions, various nonparametric approaches have been developed. In the univariate setting, rank-based distribution-free tests (Pettitt, 1979; Lombard, 1987; Einmahl and McKeague, 2003) and permutation tests (Antoch and Hušková, 2001) are well established. In the multivariate context, Chen and Zhang (2015) presented a distribution-free graph-based test, while Lung-Yut-Fong et al. (2015) enhanced rank-based methods by aggregating component-wise rank statistics using the  $L_2$ -norm, both offering asymptotic guarantees. For high-dimensional data, Yu and Chen (2022) employed the  $L_\infty$ -norm with critical values derived from bootstraps. More recently, permutation-based techniques have been heuristically incorporated into distance-based (Matteson and James, 2014) and classifier-based (Londschieen et al., 2023) methods for multivariate data. Despite these advances, adapting nonparametric changepoint detection methods to supervised scenarios—such as detecting changes in regression coefficients—remains challenging, especially in flexible, high- or infinite-dimensional settings.

The overview highlights a crucial, yet largely unresolved question in changepoint analysis: Is it feasible to devise an exact, distribution-free test that accommodates a broad class of changepoint models under minimal assumptions on the underlying data? Furthermore, can such a framework deliver effective changepoint localization and facilitate reliable subsequent inference?

## 1.1 Our contributions

In this work, we introduce a simple yet effective framework, Aggregation based on Ranks of Transformed sequences (abbreviated as ART), for changepoint detection and inference. Our methodology begins by transforming the original observations  $\{Z_i : i \in [n]\}$ —each potentially residing in an arbitrary space—into real-valued scores  $\{S_i : i \in [n]\}$ , where  $[n] = \{1, \dots, n\}$ . This transformation is *symmetric* in the sense that it does not depend on the order of the observations, thereby rendering the scores *exchangeable* in the absence of changepoints. A central component of the ART test is the ranking of these scores, where under the null hypothesis, the ranks  $\{R_i : i \in [n]\}$  are uniformly distributed over all permutations of  $[n]$ , independent of the data’s underlying distribution. We then apply an aggregation function

$\mathbb{A}$  to these ranks, yielding a test statistic  $\mathbb{A}(R_1, \dots, R_n)$ , with larger values indicating a rejection of the null hypothesis. Thanks to the distribution-free nature of the ranks, the null distribution of this statistic can be determined exactly. ART possesses several key features for changepoint testing:

- **Assumption-lean and model-agnostic:** ART imposes minimal conditions on the data-generating process (namely, independence) and applies broadly to diverse changepoint models and parameters of interest.
- **Distribution-free and exact:** The null distribution relies solely on the uniform distribution over all permutations of  $[n]$ . Consequently, the ART test is exact, ensuring valid control of the Type-I error under finite-sample scenarios.

We further outline general recipes for creating transformed scores—e.g., through *deviance* and *clustering* transformations—and describe appropriate aggregation functions, including *rank CUSUM* and *nonparametric likelihood* aggregations. These ideas accommodate high- or infinite-dimensional parameters estimated via flexible statistical/machine learning methods, where designing valid tests can be difficult.

More importantly, ART ingeniously extends to multi-scale settings, enabling multiple changepoint estimation and post-detection inference. Specifically, by locally ranking the scores and performing aggregations over multiple prespecified intervals  $\{\mathcal{I}_\ell : \ell \in [L]\}$ , we form an array of statistics  $T_{n,\ell} = \mathbb{A}(\{R_{i,\mathcal{I}_\ell}\}_{i \in \mathcal{I}_\ell})$  for  $\ell \in [L]$ , where  $R_{i,\mathcal{I}}$  denotes the rank of  $S_i$  among  $\{S_j : j \in \mathcal{I}\}$ . Despite their shared dependence on the same underlying scores, these statistics exhibit two critical properties: (i) They are jointly distribution-free if the entire dataset contains no changepoints, and (ii) Even if some intervals contain true changepoints, the joint distribution of any sub-collection of intervals that lie within homogeneous segments is the same as it would be in the absence of any changepoints, even though these intervals may individually exhibit distinct distributions. We refer to property (ii) as *pivotalness to changes*. These properties are crucial in demonstrating that ART retains its distribution-free and model-agnostic attributes, enabling finite-sample control over certain global error rates. A schematic of the procedure and key use-cases is presented in Figure 1.

## ART: Aggregation based on Ranks of Transformed sequences

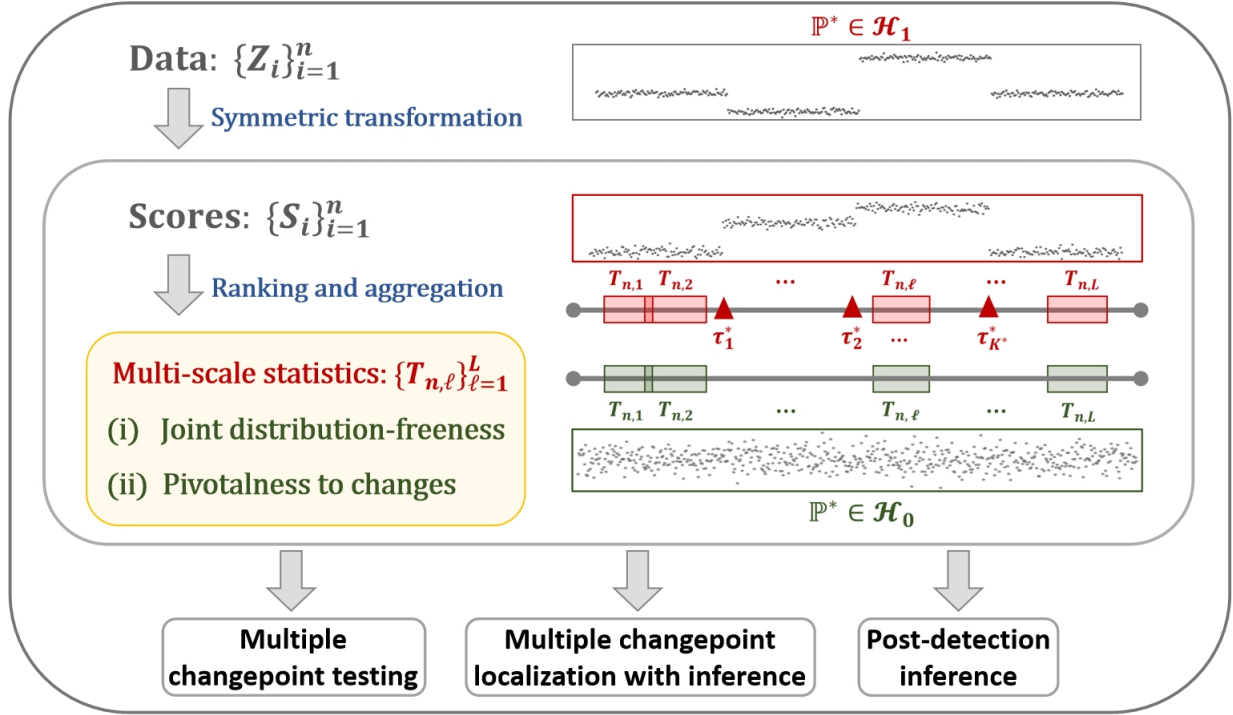


Figure 1: A flowchart illustrating the procedure, key properties, and application scenarios of ART. Here,  $\mathbb{P}^* \in \mathcal{H}_1$  characterizes the actual data distribution with changepoints  $\{\tau_k^*\}_{k \in [K^*]}$ , while  $\mathbb{P}^* \in \mathcal{H}_0$  represents a hypothetical context without any changepoints; see Section 2.1.

## 1.2 Related literature

The ART test is distribution-free and exact, properties shared by classical nonparametric methods such as permutation tests (Lehmann and Romano, 2021) and rank tests (Lehmann and D’Abrera, 1975). A permutation test involves a data-dependent critical value for a test statistic, where the null distribution remains invariant under permutations of the data. In contrast, rank tests typically yield a data-independent, exactly determinable critical value, as the null distribution is fully specified and does not depend on the data. Both approaches have a long history in changepoint testing, although much of the existing literature has focused on large-sample considerations (Pettitt, 1979; Einmahl and McKeague, 2003; Antoch and Hušková, 2001; Chen and Zhang, 2015). In this work, we integrate rank-based methods with recent advancements in randomized permutation techniques (Vovk et al., 2003; Hemerik

and Goeman, 2018), ensuring both exactness and computational feasibility for changepoint detection. Moreover, our transformation framework extends beyond univariate data, enabling the detection of general distributional changes or specific parametric shifts.

The model-agnostic and distribution-free features of ART, along with the use of transformed scores, resonate with those employed in conformal prediction (Vovk et al., 2005; Lei et al., 2018; Angelopoulos et al., 2024). Both approaches are grounded in the principle of exchangeability. While conformal prediction focuses on quantifying prediction uncertainty for independent and identically distributed (iid) data, ART aims to control error rates associated with changepoint detection which distinguishes our transformation objectives from existing works (see Section 2.2). Surprisingly, despite the non-iid nature of data in changepoint analysis, the combination of exchangeability-based rank statistics with multi-scale aggregations provide finite-sample guarantees.

Expanding on the “pivotalness to changes” property, ART integrates seamlessly with contemporary developments in uncertainty quantification for changepoint analysis (Fryzlewicz, 2024a; Jia et al., 2024). This integration not only strengthens the contributions of these methods but also capitalizes on ART’s inherent attributes of being distribution-free, model-agnostic, and capable of handling finite samples effectively.

### 1.3 Structure and notations

The remainder of this paper is structured as follows. Section 2 outlines the main ideas behind the ART framework, focusing on the notions of symmetric transformation, ranking and aggregations, and their multi-scale extensions. Section 3 delves into its application in multiple changepoint testing, localization with inference, and post-detection inference, particularly emphasizing the error rate control throughout these procedures. Simulation studies and real-data analyses are detailed in Section 4. Section 5 concludes the paper. All theoretical proofs, together with additional algorithmic and numerical details, are provided in the supplementary material.

**Notations:** The indicator function is denoted by  $\mathbb{1}\{\cdot\}$ . The cardinality of set  $A$  is given by  $|A|$ . Let  $\|\cdot\|_2$  and  $\|\cdot\|_\infty$  denote the  $L_2$ - and  $L_\infty$ -norms, respectively. For any  $x \in \mathbb{R}$ , let

$\lfloor x \rfloor$  denote the greatest integer no larger than  $x$ . For random variables  $X$  and  $Y$ ,  $X \stackrel{d}{=} Y$  indicates equality in distribution. The uniform distribution over  $[0, 1]$  is denoted by  $\mathcal{U}(0, 1)$ , and  $\mathcal{U}(\Pi_n)$  represents the uniform distribution over all permutations of  $[n]$ , each permutation  $\pi$  having an equal probability of  $1/n!$ .

## 2 ART methodology and key principles

### 2.1 Data and changepoint model

Consider a sequence of independent observations  $\mathcal{D} = (Z_1, \dots, Z_n)$ , where each observation takes values in a space  $\mathcal{Z}$ . Let  $\mathbb{P}^*$  denote the true joint distribution of the data.

Suppose that there are  $K^* \geq 0$  changepoints at locations  $0 \equiv \tau_0^* < \tau_1^* < \dots < \tau_{K^*}^* < \tau_{K^*+1}^* \equiv n$ , partitioning the sequence into  $K^* + 1$  segments. Within each segment  $k \in [K^* + 1]$ , the observations  $\{Z_i : i \in (\tau_{k-1}^*, \tau_k^*]\}$  are identically distributed according to a distribution  $P_k^*$ , with  $P_{k+1}^* \neq P_k^*$  for  $k \in [K^*]$ . In situations where distributional changes can be described by a specific parameter, we express  $P_k^* = P_{\theta_k^*}$ , where  $\theta_{k+1}^* \neq \theta_k^*$  for  $k \in [K^*]$ . Specific examples include:

**Example 1** (Changes in means). Let  $\mathcal{Z} = \mathbb{R}^d$ , and  $Z_i = \theta_k^* + \varepsilon_i$  for  $i \in (\tau_{k-1}^*, \tau_k^*]$ , where  $\varepsilon_i$  are iid from  $P_\epsilon$ . Here,  $P_{\theta_k^*}(z) = P_\epsilon(z - \theta_k^*)$ .

**Example 2** (Changes in regression coefficients). Let  $z = (y, x) \in \mathcal{Z} = \mathbb{R} \times \mathbb{R}^d$ , and  $y_i = x_i^\top \theta_k^* + \varepsilon_i$  for  $i \in (\tau_{k-1}^*, \tau_k^*]$ , where the covariates  $x_i$  are iid from  $P_x$ , the noises  $\varepsilon_i$  are iid from  $P_\epsilon$ , and the covariates and noises are independent. Here,  $P_{\theta_k^*}(z) = P_x \cdot P_\epsilon(y - x^\top \theta_k^*)$ .

Let  $\mathcal{P}$  denote the set of all distributions over  $\mathcal{Z}$ . Define  $\mathcal{H}_0 = \{P_1^n : P_1 \in \mathcal{P}\}$  as the set of distributions in the absence of any changepoints (i.e.,  $K^* = 0$ ). Conversely, define  $\mathcal{H}_1 = \{\prod_{k \in [K^*+1]} P_k^{\tau_k^* - \tau_{k-1}^*} : P_k \in \mathcal{P}, P_{k+1} \neq P_k \text{ for } k \in [K^*]\}$  for distributions with  $K^* > 0$  changepoints at specified locations.

## 2.2 Transformation

Our methodology begins by transforming the observations into *scores*  $S_i = \mathbb{S}(Z_i; \mathcal{D})$ , where  $\mathbb{S}$  is a *symmetric* transformation function, defined as follows:

**Definition 1** (Symmetric transformation). *A transformation function  $\mathbb{S} : \mathcal{Z} \times \mathcal{Z}^n \rightarrow \mathbb{R}$  is symmetric if for any  $z \in \mathcal{Z}$  and any permutation  $\pi$  on  $[n]$ ,  $\mathbb{S}(z; \mathcal{D}) = \mathbb{S}(z; \mathcal{D}_\pi)$ , where  $\mathcal{D}_\pi = (Z_{\pi(1)}, \dots, Z_{\pi(n)})$ .*

This transformation is designed to generate scores that can reflect potential changepoints within the data. We introduce two general transformation approaches:

- *Deviance transformation:*  $\mathbb{S}(z; \mathcal{D}) = \mathbb{D}(z; \hat{f}_{\mathcal{D}})$ , which quantifies the deviation of an observation  $z$  from a baseline model  $\hat{f}_{\mathcal{D}}$  trained on  $\mathcal{D}$ . We require  $\hat{f}_{\mathcal{D}} = \hat{f}_{\mathcal{D}_\pi}$  for any permutation  $\pi$  on  $[n]$ , ensuring the symmetry of  $\mathbb{S}(z; \mathcal{D})$ . For instance, in Example 2, a practical choice is  $\mathbb{D}(z; \hat{f}_{\mathcal{D}}) = (y - x^\top \hat{\theta}_{\mathcal{D}})^2$ , where  $\hat{\theta}_{\mathcal{D}}$  is a prespecified or estimated regression coefficients. In Example 1, one can use  $\mathbb{D}(z; \hat{f}_{\mathcal{D}}) = -p_{\hat{\theta}_{\mathcal{D}}}(z)$ , where  $p_{\theta}(z)$  represents a predefined parametric density  $p_{\theta}(\cdot)$  evaluated at  $z$  and  $\hat{\theta}_{\mathcal{D}}$  is a prespecified or estimated parameter.

This approach is conceptually similar to the conformal score function used in conformal prediction (e.g., Angelopoulos et al., 2024), where each score quantifies the discrepancy between the true response (or a hypothetical one) and the model’s prediction. We anticipate that changes in the original data will manifest as corresponding changes in the transformed scores, whether in location or distribution.

- *Clustering transformation:*  $\mathbb{S}(z; \mathcal{D}) = \mathbb{C}(z; \hat{f}_{\mathcal{D}})$ , which employs a clustering algorithm  $\hat{f}_{\mathcal{D}}$  to assign a unique integer label to each observation  $z$ . Again, we require  $\hat{f}_{\mathcal{D}} = \hat{f}_{\mathcal{D}_\pi}$  for any permutation  $\pi$  on  $[n]$ . Suitable clustering algorithms include  $K$ -means, hierarchical clustering, density-based clustering, and spectral clustering. When specifying the number of clusters, strategies that are invariant to the order of data, such as the heuristic elbow method, the gap statistic (Tibshirani et al., 2001), or certain information criteria, should be employed.



Further details and examples are provided in Table 1 in Section 4. For changepoint analysis involving high-dimensional and non-Euclidean data (Chen and Chu, 2023; Londschieen et al., 2023; Li et al., 2024), variable selection and dimension reduction techniques that remain invariant to data order are applicable, prior to any transformation. A detailed transformation approach employing deep embedded clustering (Xie et al., 2016) for such data is provided in Algorithm S.2 in the supplementary material.

## 2.3 Ranking and aggregation

We outline our methodology for detecting the presence of changepoints. Formally, we test the null hypothesis  $H_0 : \mathbb{P}^* \in \mathcal{H}_0$  against the alternative  $H_1 : \mathbb{P}^* \in \mathcal{H}_1$ . Let  $\Pr$  be the probability evaluated considering all random quantities, and  $\Pr_{H_0}$  evaluates  $\Pr$  under  $H_0$ .

Under  $H_0$ , the symmetric transformation renders the scores *exchangeable*:

$$(S_1, \dots, S_n) \stackrel{d}{=} (S_{\pi(1)}, \dots, S_{\pi(n)}),$$

for any permutation  $\pi$  on  $[n]$ . A key component of our test involves the *ranking* of these scores. The rank of each score  $S_i$  for  $i \in [n]$  among  $\{S_j : j \in [n]\}$  is defined as:

$$R_i \equiv R_{i,[n]} = |\{j \in [n] : S_j \leq S_i\}|.$$

To break ties in the ranks, particularly common with clustering transformations, we modify the scores to  $S_i + \epsilon e_i$ , where  $\epsilon > 0$  is a small constant (e.g.,  $\epsilon = 10^{-6}$ ) and  $\{e_i : i \in [n]\}$  are iid  $\mathcal{N}(0, 1)$  random variables. Under  $H_0$ ,  $(R_1, \dots, R_n)$  follows the uniform distribution over all permutations of  $[n]$ , namely  $\mathcal{U}(\Pi_n)$ . Our test *aggregates* these ranks using a function  $\mathbb{A} : [n]^n \rightarrow \mathbb{R}$ , with larger values of the test statistic  $T_n = \mathbb{A}(R_1, \dots, R_n)$  indicating evidence against  $H_0$ . This method is referred to as “Aggregation based on Ranks of Transformed sequences” (ART).

We present two practical aggregation functions:

- *Rank cumulative sum (CUSUM) aggregation*:

$$\mathbb{A}(R_1, \dots, R_n) = n^{-3/2} \sup_{1 \leq t < n} \left| \sum_{i=1}^t (R_i - \bar{R}_n) \right|,$$

where  $\bar{R}_n = n^{-1} \sum_{i=1}^n R_i = (n+1)/2$ . This aggregation is equivalent to computing the maximum of the sequence of the absolute vales of Wilcoxon-Mann-Whitney two-sample statistics  $n^{-3/2} \sum_{i=1}^t \sum_{j=t+1}^n \{\mathbb{1}(S_j \leq S_i) - 1/2\}$  over  $1 \leq t < n$ . For observations  $Z_i \in \mathbb{R}$  and scores  $S_i = Z_i$ , this test statistic is identical to the one proposed by [Pettitt \(1979\)](#).

- *Nonparametric likelihood aggregation:*

$$\mathbb{A}(R_1, \dots, R_n) = \sup_{1 \leq t < n} 2 \int_{s \in \mathbb{R}} \Lambda([t], [n] \setminus [t]; s) \widehat{F}_{[n]}(s)^{-1} \{1 - \widehat{F}_{[n]}(s)\}^{-1} d\widehat{F}_{[n]}(s),$$

where  $\widehat{F}_{\mathcal{I}}(s) = (|\mathcal{I}| + 1)^{-1} \{\sum_{i \in \mathcal{I}} \mathbb{1}(S_i \leq s) + 0.5\}$  denotes the empirical distribution function of the scores  $\{S_i : i \in \mathcal{I}\}$ , adjusted for continuity, and

$$\begin{aligned} \Lambda(\mathcal{I}_1, \mathcal{I}_2; s) = & |\mathcal{I}_1| \left[ \widehat{F}_{\mathcal{I}_1}(s) \log \frac{\widehat{F}_{\mathcal{I}_1}(s)}{\widehat{F}_{\mathcal{I}}(s)} + \{1 - \widehat{F}_{\mathcal{I}_1}(s)\} \log \frac{1 - \widehat{F}_{\mathcal{I}_1}(s)}{1 - \widehat{F}_{\mathcal{I}}(s)} \right] \\ & + |\mathcal{I}_2| \left[ \widehat{F}_{\mathcal{I}_2}(s) \log \frac{\widehat{F}_{\mathcal{I}_2}(s)}{\widehat{F}_{\mathcal{I}}(s)} + \{1 - \widehat{F}_{\mathcal{I}_2}(s)\} \log \frac{1 - \widehat{F}_{\mathcal{I}_2}(s)}{1 - \widehat{F}_{\mathcal{I}}(s)} \right] \end{aligned}$$

represents the nonparametric likelihood ratio statistic for evaluating distributional equality of two samples  $\{S_i : i \in \mathcal{I}_1\}$  and  $\{S_i : i \in \mathcal{I}_2\}$  ([Zhang, 2006](#)), with  $\mathcal{I} = \mathcal{I}_1 \cup \mathcal{I}_2$ .

For independent observations  $Z_i \in \mathbb{R}$  and scores  $S_i = Z_i$ , the rank CUSUM aggregation is renowned for its effectiveness in detecting locational changes within the scores. To capture other types of changes such as scale shifts, extensions employing linear rank statistics can be developed ([Lombard, 1987](#)). Alternatively, we suggest the nonparametric likelihood aggregation, which is advantageous for detecting omnibus distributional changes. These aggregations rely solely on the ranks of the scores, ensuring their exact distribution-freeness under  $H_0$ . This property holds true for exchangeable scores in our scenarios, which are transformed from general objects  $Z_i \in \mathcal{Z}$  and may be highly dependent.

The corresponding null distribution or p-value can be determined exactly through the enumeration of all  $n!$  permutations, which, however, becomes computationally prohibitive for large  $n$ . The literature often turns to asymptotic distributions for univariate data ([Hušková, 1997](#)). Here, we propose a *randomized* p-value inspired by conformal prediction methodologies (e.g. [Vovk et al., 2003](#)):

$$p_B = \frac{\sum_{b=1}^B \mathbb{1}\{\mathbb{A}(\pi_b) > T_n\} + U [1 + \sum_{b=1}^B \mathbb{1}\{\mathbb{A}(\pi_b) = T_n\}]}{B + 1},$$

where  $\pi_1, \dots, \pi_B$  are iid from  $\mathcal{U}(\Pi_n)$ , and  $U \sim \mathcal{U}(0, 1)$  serves to break ties.

**Theorem 1.** *Under  $H_0$ , with symmetric transformations: (i)  $T_n \stackrel{d}{=} \mathbb{A}(\pi)$ , where  $\pi \sim \mathcal{U}(\Pi_n)$ ; (ii)  $p_B \sim \mathcal{U}(0, 1)$  for any  $B > 0$ .*

Theorem 1 confirms the exact validity of the p-value  $p_B$ . Given a prespecified nominal level  $\alpha \in (0, 1)$ , we reject  $H_0$  if  $p_B < \alpha$ . The validity of this p-value is exactly upheld regardless of the parameter  $B$ . In practice, we recommend a default value of  $B = 200$ .

**Example 2** (Revisited; High-dimensional setting). *Testing for a change in regression coefficients when  $d \gg n$  presents significant challenges. Recently, Zhao et al. (2024) introduced a bias-corrected quadratic-form-based CUSUM (QF-CUSUM) test that uses separate LASSO fits at each candidate changepoint, along with a randomization strategy to maintain non-degeneracy under the null hypothesis. ART provides simple alternatives: (i) a deviance transformation (with a single global LASSO fit  $\hat{\theta}_{\mathcal{D}}$ , see Table 1), followed by a nonparametric likelihood aggregation; (ii) a standard  $K$ -means clustering transformation (see Algorithm S.1 in the supplementary material) applied to the data after discarding all inactive features (those with zero components of  $\hat{\theta}_{\mathcal{D}}$ ), followed by a rank CUSUM aggregation. Both implementations guarantee exact size control and demonstrate competitive power (see Section 4.1).*

## 2.4 Multi-scale adaptations

We expand the ideas of ranking and aggregation into a multi-scale framework, laying the groundwork for discussions on multiple changepoint testing, localization, and post-detection inference in Section 3. This framework involves a sequence of  $L$  prespecified intervals  $\{\mathcal{I}_\ell \subset (0, n] : \ell \in [L]\}$ , which may overlap.

Given the transformed scores  $\{S_i : i \in [n]\}$ , the *local* rank of  $S_i$  within a specific interval  $\mathcal{I}_\ell$ , for  $i \in \mathcal{I}_\ell$  and  $\ell \in [L]$ , is defined as:

$$R_{i,\ell} \equiv R_{i,\mathcal{I}_\ell} = |\{j \in \mathcal{I}_\ell : S_j \leq S_i\}|.$$

At each interval, these local ranks are aggregated to construct the statistic  $T_{n,\ell} = \mathbb{A}(\{R_{i,\ell} : i \in \mathcal{I}_\ell\})$ . This *multi-scale* local aggregations result in a sequence of statistics  $\{T_{n,\ell} : \ell \in [L]\}$ .

According to Theorem 1, each statistic  $T_{n,\ell}$  exhibits a marginally distribution-freeness property under  $H_0$ . However, analyzing the joint distribution of  $(T_{n,1}, T_{n,2}, \dots, T_{n,L})$  under  $H_0$  presents significant challenges due to potential complex dependency among scores and overlapped intervals.

**Theorem 2.** *With symmetric transformations and data-independent intervals  $\{\mathcal{I}_\ell\}_{\ell=1}^L$ :*

- (i) *(Joint distribution-freeness) Under  $H_0$ ,  $(T_{n,1}, T_{n,2}, \dots, T_{n,L}) \stackrel{d}{=} \mathbb{G}(\pi)$  for a function  $\mathbb{G} : [n] \rightarrow \mathbb{R}^L$ , where  $\pi \sim \mathcal{U}(\Pi_n)$ , and thus its joint distribution is independent of the underlying distribution  $P_1^*$ .*
- (ii) *(Pivotalness to changes) If no changepoints are present within any interval  $\mathcal{I}_\ell$ , the joint distribution of  $(T_{n,1}, T_{n,2}, \dots, T_{n,L})$  is invariant under both  $H_0$  and  $H_1$ .*

Theorem 2 is based on a critical observation: The relational ordering between any two scores is directly mirrored in their respective ranks within any given interval. Consequently, we have  $R_{i,\ell} = |\{j \in \mathcal{I}_\ell : R_j \leq R_i\}|$ , which leads to the property of joint distribution-freeness under  $H_0$ . Similarly, if  $\mathcal{I}_\ell \subset (\tau_{k-1}^*, \tau_k^*]$  for some  $k \in [K^* + 1]$ , then  $R_{i,\ell} = |\{j \in \mathcal{I}_\ell : R_{j,(\tau_{k-1}^*, \tau_k^*]} \leq R_{i,(\tau_{k-1}^*, \tau_k^*]} \}|$ . This supports the pivotalness property, further reinforced by the independence of  $\{R_{i,(\tau_{k-1}^*, \tau_k^*]} : i \in (\tau_{k-1}^*, \tau_k^*]\}$  across all true segments  $k$ . Further details and proofs can be found in the supplementary material.

Building on Theorem 2(i), under  $H_0$ ,  $\max_{\ell \in [L]} T_{n,\ell} \stackrel{d}{=} \|\mathbb{G}(\pi)\|_\infty$ . For any  $\alpha \in (0, 1)$ , define:

$$t_{\alpha,B} = \text{the } [(1 - \alpha)(B + 1)]\text{-st smallest value among } \{\|\mathbb{G}(\pi_b)\|_\infty : b \in [B]\}, \quad (1)$$

where  $\pi_1, \dots, \pi_B$  are iid from  $\mathcal{U}(\Pi_n)$ .

**Corollary 1.** *With symmetric transformations and data-independent intervals  $\{\mathcal{I}_\ell\}_{\ell=1}^L$ , under  $H_0$ ,  $\Pr \{\max_{\ell \in [L]} T_{n,\ell} > t_{\alpha,B}\} \leq \alpha$  for any  $\alpha \in (0, 1)$  and  $B > 0$ .*

### 3 Multiple changepoint analysis

This section builds upon the multi-scale principles established in Theorem 2 to broaden the scope of the proposed ART method across a series of tasks within multiple changepoint

analysis. These tasks include multiple changepoint testing, localization with inference, and post-detection inference, while maintaining control over specific global error rates. The enhancements preserve the model-agnostic and distribution-free attributes of the ART test, ensuring finite-sample guarantees.

### 3.1 Multiple changepoint testing

As discussed in Section 2.3, the ART test employs the statistic  $T_n = \mathbb{A}(R_1, \dots, R_n)$ , through aggregations typically using a binary search to identify the most significant locational or distributional changes. This framework is well-suited for scenarios involving at most one change (AMOC). However, its performance tends to diminish in the presence of multiple changepoints, reflecting similar limitations observed with binary segmentation estimation procedures in these contexts (Fryzlewicz, 2014). To address this issue we propose a multi-scale ART test specifically configured for assessing the presence of multiple changepoints.

Utilizing the multi-scale framework outlined in Section 2.4, we engage a sequence of prespecified intervals  $\{\mathcal{I}_\ell : \ell \in [L]\}$ . From these intervals, we construct a sequence of statistics  $\{T_{n,\ell} : \ell \in [L]\}$  and use the maximum of these statistics

$$T_{n,\text{multi}} = \max_{\ell \in [L]} T_{n,\ell}$$

as our test statistic. The approach aims to include segments that, by chance, revert to the AMOC scenario where the statistic  $T_{n,\ell}$  proves effective. The selection of intervals may employ moving windows (Niu and Zhang, 2012; Eichinger and Kirch, 2018), scanning techniques (Chan and Walther, 2013), random selection from  $(0, n]$  (Fryzlewicz, 2014), or through deterministic strategies within  $(0, n]$  (Kovács et al., 2023).

Given  $T_{n,\text{multi}} \stackrel{d}{=} \|\mathbb{G}(\pi)\|_\infty$ , where  $\pi \sim \mathcal{U}(\Pi_n)$ , the associated p-value is readily accessible:

$$p_{B,\text{multi}} = \frac{\sum_{b=1}^B \mathbb{1}\{\|\mathbb{G}(\pi_b)\|_\infty > T_{n,\text{multi}}\} + U[1 + \sum_{b=1}^B \mathbb{1}\{\|\mathbb{G}(\pi_b)\|_\infty = T_{n,\text{multi}}\}]}{B + 1},$$

where  $\pi_1, \dots, \pi_B$  are iid from  $\mathcal{U}(\Pi_n)$  and  $U \sim \mathcal{U}(0, 1)$ . We reject the null hypothesis  $H_0$  when  $p_{B,\text{multi}} < \alpha$ , given a prespecified nominal Type-I error  $\alpha \in (0, 1)$ .

**Theorem 3.** *With symmetric transformations and data-independent intervals  $\{\mathcal{I}_\ell\}_{\ell=1}^L$ , under  $H_0$ ,  $\Pr\{p_{B,\text{multi}} < \alpha\} = \alpha$  for any  $\alpha \in (0, 1)$  and  $B > 0$ .*

### 3.2 Multiple changepoint localization with inference

Once  $H_0$  is rejected, the subsequent task is to localize multiple changepoints. Recently, Narrowest Significance Pursuit (NSP; Fryzlewicz, 2024a) has been introduced to identify localized regions exhibiting change while maintaining global significance control; see also Fang et al. (2020). However, these methods often assume specific models (e.g., univariate mean shifts or changes in linear regression coefficients) and rely on known error distributions, limiting their applicability in more general contexts.

To overcome these limitations, we integrate the ART methodology with the NSP paradigm. This integration preserves the model-agnostic and distribution-free nature of ART, while maintaining finite-sample control over global false positive rates. The detailed algorithm is presented in Algorithm 1.

This algorithm employs a recursive function  $\text{NOT}(s, e, t_{\alpha, B})$  (see Line 4), inspired by the Narrowest-Over-Threshold (NOT; Baranowski et al., 2019) procedure, to identify the narrowest sub-interval  $\mathcal{I}_{\hat{\ell}}$  for which the statistic  $T_{n, \hat{\ell}}$  exceeds a prespecified threshold  $t_{\alpha, B}$  (see Line 10). Although NOT provides large-sample consistency for changepoint estimation with appropriate thresholds, it does not quantify estimation uncertainty. NSP complements NOT for a broad class of linear models by identifying a set of regions, with high probability, each containing at least one true changepoint, thus controlling the global false positive rate. NSP achieves this via a multisolution sup-norm loss-based statistic that measures deviations from linearity, with the threshold determined through simulation assuming a known error distribution. In contrast, ART localization is model-agnostic, avoiding linearity assumptions. It remains distribution-free, determining the threshold independently of the data. In practice, the intervals used in the ART localization algorithm can be chosen deterministically (e.g., all sub-intervals of  $(0, n]$ , a sparse set of dyadic intervals (Fryzlewicz, 2024a), or seeded intervals (Kovács et al., 2023)), or selected randomly (Fryzlewicz, 2014; Baranowski et al., 2019), offering flexibility in different settings.

**Theorem 4.** *With symmetric transformations and data-independent intervals  $\{\mathcal{I}_{\ell}\}_{\ell=1}^L$ , for any  $\alpha \in (0, 1)$ ,  $\Pr \{ \text{there exists } \hat{R} \in \hat{\mathcal{R}} \text{ such that } \hat{R} \cap \mathcal{T}^* = \emptyset \} \leq \alpha$ , where  $\mathcal{T}^* = \{\tau_1^*, \dots, \tau_{K^*}^*\}$ .*

Theorem 4 establishes that the ART localization achieves finite-sample control of the

---

**Algorithm 1:** ART localization algorithm.

---

**Input:** Observations  $\mathcal{D} = \{Z_i : i \in [n]\}$ ; symmetric transformation  $\mathbb{S}$ ; rank aggregation  $\mathbb{A}$ ; data-independent intervals  $\{\mathcal{I}_\ell : \ell \in [L]\}$ ; and any algorithm SCP to locate a single changepoint.

- 1 *Transformation:* Compute scores  $S_i = \mathbb{S}(Z_i; \mathcal{D})$  for  $i \in [n]$ .
- 2 *Multi-scale ranking and aggregation:* Construct statistics  $T_{n,\ell} = \mathbb{A}(\{R_{i,\ell} : i \in \mathcal{I}_\ell\})$  for  $\ell \in [L]$ , as described in Section 2.4.
- 3 *Localization:* Initialize  $\widehat{\mathcal{R}} = \emptyset$  and  $\widehat{\mathcal{T}} = \emptyset$ . Execute  $\text{NOT}(1, n, t_{\alpha,B})$  with threshold  $t_{\alpha,B}$  defined in Eq. (1).

4 **Function**  $\text{NOT}(s, e, t_{\alpha,B})$ :

```
5   if  $e - s \leq 1$ , then STOP
6   else
7      $\mathcal{L}_{s,e} = \{\ell : \mathcal{I}_\ell \subset [s, e]\}$ 
8     if  $\mathcal{L}_{s,e} = \emptyset$ , then STOP
9     else
10       $\mathcal{L}_{s,e}^+ := \{\ell \in \mathcal{L}_{s,e} : T_{n,\ell} > t_{\alpha,B}\}$ 
11      if  $\mathcal{L}_{s,e}^+ = \emptyset$ , then STOP
12      else
13         $\widehat{\ell} = \arg \min_{\ell \in \mathcal{L}_{s,e}^+} |\mathcal{I}_\ell|$ ; denote  $\mathcal{I}_{\widehat{\ell}} = [s_{\widehat{\ell}}, e_{\widehat{\ell}}]$ 
14        Estimate a changepoint  $\widehat{\tau}$  within  $\mathcal{I}_{\widehat{\ell}}$  via SCP (see Section 3.2.1)
15        Update  $\widehat{\mathcal{R}} = \widehat{\mathcal{R}} \cup \{\mathcal{I}_{\widehat{\ell}}\}$  and  $\widehat{\mathcal{T}} = \widehat{\mathcal{T}} \cup \{\widehat{\tau}\}$ 
16         $\text{NOT}(s, s_{\widehat{\ell}}, t_{\alpha,B})$ 
17         $\text{NOT}(e_{\widehat{\ell}}, e, t_{\alpha,B})$ 
```

**Output:** Localized regions  $\widehat{\mathcal{R}}$  and estimated changepoints  $\widehat{\mathcal{T}}$ .

---

global false positive rate, extending the principle behind NSP into a model-agnostic and distribution-free context. The proof can be outlined as follows:

$$\Pr \{ \text{there exists } \widehat{R} \in \widehat{\mathcal{R}} \text{ such that } \widehat{R} \cap \mathcal{T}^* = \emptyset \}$$

$$\begin{aligned}
&\stackrel{(i)}{\leq} \Pr \left\{ \max_{\ell \in [L]; \mathcal{I}_\ell \cap \mathcal{T}^* = \emptyset} T_{n,\ell} > t_{\alpha,B} \right\} \\
&\stackrel{(ii)}{=} \Pr_{H_0} \left\{ \max_{\ell \in [L]; \mathcal{I}_\ell \cap \mathcal{T}^* = \emptyset} T_{n,\ell} > t_{\alpha,B} \right\} \stackrel{(iii)}{\leq} \Pr_{H_0} \left\{ \max_{\ell \in [L]} T_{n,\ell} > t_{\alpha,B} \right\} \stackrel{(iv)}{\leq} \alpha.
\end{aligned}$$

Inequality (i) leverages the construction of the NOT-based localization algorithm. Equality (ii) applies the pivotalness property from Theorem 2(ii), transferring from  $\Pr$  to  $\Pr_{H_0}$ , thus ensuring a model-agnostic perspective. Inequality (iii) relaxes the subset of intervals to all intervals. Finally, Inequality (iv) follows from Corollary 1, which ensures distribution-free thresholding. In contrast to NSP, where global false positive rate control relies on linearity assumptions and known error distributions, the pivotalness in equality (ii) and the distribution-free threshold determination in inequality (iv) enable ART to achieve finite-sample control without imposing such restrictions.

### 3.2.1 Changepoint estimation consistency

The ART localization algorithm produces a set of estimated changepoints from the narrowest intervals  $\mathcal{I}_{\hat{\tau}_\ell}$  (see Line 14). The estimation algorithm SCP used can be flexibly chosen, such as simply returning the midpoint of each interval (Fryzlewicz, 2024a), or in a model-assisted way. To keep the ART framework self-contained, we employ an approach based on the aggregation function that seeks to maximize statistics reflecting locational or distributional deviations. For instance, consider the rank CUSUM aggregation applied to an interval  $\mathcal{I}_\ell \equiv [s_\ell, e_\ell]$ , and define the estimated changepoint as  $\hat{\tau}_\ell = \arg \max_{s_\ell \leq t < e_\ell} |\mathcal{I}_\ell|^{-3/2} \left| \sum_{i=s_\ell}^t \sum_{j=t+1}^{e_\ell} \mathbb{1}(S_j \leq S_i) - 1/2 \right|$ .

We investigate the consistency of the estimated changepoints through the rates at which the lengths of these intervals contract. For clarity, we focus on the deviance transformation  $\mathbb{S}(z; \mathcal{D}) = \mathbb{D}(z; \hat{f}_{\mathcal{D}})$ , where  $\hat{f}_{\mathcal{D}}$  is a baseline model that is either prespecified or estimated from the entire data over a model space  $\mathcal{F}$ . Under the multi-scale ranking and aggregation framework, we consider all sub-intervals of  $(0, n]$  and apply the rank CUSUM aggregation. For  $k \in [K^*]$ , with  $Z_i \sim P_k^*$  and  $Z_j \sim P_{k+1}^*$ , define  $Q_k(f) = \Pr\{\mathbb{D}(Z_j; f) \leq \mathbb{D}(Z_i; f)\} - 1/2$ , which measures the signal of the change between adjacent segments relative to a candidate model  $f \in \mathcal{F}$ . Let  $\|\cdot\|_{\mathcal{F}}$  denote the norm induced by the model space  $\mathcal{F}$ .



**Assumption 1.** (i) (Baseline model) There exists an  $f_0 \in \mathcal{F}$  and a constant  $c_1 > 0$  such that  $\Pr\{\|\widehat{f}_{\mathcal{D}} - f_0\|_{\mathcal{F}} \leq c_1 \sqrt{(\log n)/n}\} = 1 + o(1)$ . (ii) (Rank function class) The class of functions  $\{h_f(z_1, z_2) : h_f(z_1, z_2) = \mathbb{1}(\mathbb{D}(z_2; f) \leq \mathbb{D}(z_1; f)) - 1/2, f \in \mathcal{F}\}$  is a Vapnik–Chervonenkis (VC) class of finite VC dimension  $\nu$ . (iii) (Change spacings) For  $k \in [K^* + 1]$ ,  $\tau_k^* - \tau_{k-1}^* \geq 2(d_k + d_{k-1})$ , where  $d_k = \lceil c_2(\log n)/\{Q_k(f_0)\}^2 \rceil + 1$  for some constant  $c_2 > 0$ , with  $d_0 = d_{K^*+1} = 0$ . (iv) (Change signal smoothness) For each  $k \in [K^*]$ ,  $Q_k(f)$  is Lipschitz continuous, i.e.,  $|Q_k(f_1) - Q_k(f_2)| \leq c_3 \|f_1 - f_2\|_{\mathcal{F}}$  for all  $f_1, f_2 \in \mathcal{F}$ , for some constant  $c_3 > 0$ .

For a prespecified baseline model  $\widehat{f}_{\mathcal{D}} = f_0$ , Assumption 1(i) holds trivially. In finite-dimensional settings, this assumption is typically satisfied under mild conditions, especially when  $\widehat{f}_{\mathcal{D}}$  is a global fit and  $f_0$  corresponds to a mixture of underlying segment models. Under simple transformations like  $\mathbb{D}(z; f) = \|z - f\|_2^2$  or  $\mathbb{D}(z, f) = -\phi(z - f)$  for a standard multivariate normal density  $\phi$ , Assumption 1(ii) follows from standard VC theory (Chapter 4, Vapnik, 1998). Assumption 1(iii) imposes a minimum spacing requirement between adjacent changepoints on the order of  $(\log n)/\min\{\{Q_k(f_0)\}^2, \{Q_{k-1}(f_0)\}^2\}$ . In the simple case where  $S_i = Z_i \in \mathbb{R}$ ,  $Q_k(f) = \Pr\{Z_j \leq Z_i\} - 1/2$  corresponds to a familiar measure for locational changes (Darkhovskh, 1976). Assumption 1(iv) requires that  $Q_k(f)$  vary smoothly as the model  $f$  changes.

**Proposition 1.** Given that Assumption 1 holds, as  $n \rightarrow \infty$ , with probability at least  $1 - \alpha + o(1)$ ,  $\widehat{\mathcal{R}}$  contains exactly  $K^*$  intervals  $[\widehat{s}_1, \widehat{e}_1] < \dots < [\widehat{s}_{K^*}, \widehat{e}_{K^*}]$  such that  $\tau_k^* \in [\widehat{s}_k, \widehat{e}_k]$  and  $\widehat{e}_k - \widehat{s}_k \leq 2d_k$  for all  $k \in [K^*]$ .

Proposition 1 parallels to the results on NSP-based localization for linear models (Fryzlewicz, 2024a), yet under a more general, model-agnostic setting. It demonstrates that the ART localization correctly identifies the number of changepoints, each interval returned contains exactly one true changepoint, and the interval length scales on the order of  $O((\log n)/Q_k(f_0)^2)$ . These findings coincide with the optimal (up to a  $\log n$  factor) nonparametric convergence rates reported for univariate changepoint detection problems (Madrid Padilla et al., 2021), despite differences in how signals are characterized.

### 3.3 Inference after multiple changepoint localization

Section 3.2 addresses the localization of regions where changepoints may occur, providing finite-sample global false positive rate control under minimal model and distributional assumptions. To identify a specific changepoint within each region, additional conditions are necessary for consistent estimation. This approach—where interval-based confidence assessments precede the actual localization—is sometimes referred to as *post-inference selection* (Fryzlewicz, 2024a). In contrast, many practical applications invoke *post-selection* or *post-detection inference*, wherein a set of changepoints is already detected by some method, and the goal is to assess their reliability. Much of the existing literature focus on detection consistency but imposes conditions that may fail in practice—particularly for flexible statistical or machine-learning-based methods. Consequently, some detected changepoints could be inaccurate or even spurious, emphasizing the need for rigorous post-detection inference (Hyun et al., 2018, 2021; Duy et al., 2020; Jewell et al., 2022; Carrington and Fearnhead, 2025).

We formalize the problem as follows. Let  $\widehat{\mathcal{T}} = \{\widehat{\tau}_j : j \in [\widehat{K}]\}$  be a set of detected changepoints, which may from any detection and localization procedures tailored for specific models. The aim is to test the following sequence of hypotheses (Jewell et al., 2022):

$$H_{0j} : P_{\widehat{\tau}_j-h+1}^* = \dots = P_{\widehat{\tau}_j+h}^* \text{ versus } H_{1j} : \text{not } H_{0j}, \quad \text{for } j \in [\widehat{K}], \quad (2)$$

where  $h > 0$  defines a prespecified window. If  $H_{0j}$  holds, indicating the absence of any true changepoint in  $(\widehat{\tau}_j - h, \widehat{\tau}_j + h]$ , then  $\widehat{\tau}_j$  is treated as a true null. Rejecting  $H_{0j}$  labels  $\widehat{\tau}_j$  as reliable, and we define the set of such reliable changepoints by  $\widehat{\mathcal{T}}_R = \{\widehat{\tau}_j \in \widehat{\mathcal{T}} : H_{0j} \text{ is rejected}\}$ .

This post-detection inference task is made difficult by the “double-dipping” phenomenon: The same data is used both to select the changepoints and to test their significance. While recent research offers selective p-values that condition on the selection process, those techniques often rely on stringent assumptions tied to specific changepoint models (e.g., Example 1 where  $P_{\theta_k^*} = \mathcal{N}(\theta_k^*, 1)$ ) and detection algorithms.

Alternatively, by recognizing the multiplicity in testing  $\{H_{0j} : j \in [\widehat{K}]\}$ , Jia et al. (2024) defines a family-wise error rate (FWER):

$$\text{FWER} \equiv \Pr \{ \text{there exists some } \widehat{\tau}_j \in \widehat{\mathcal{T}}_R \cap \mathcal{G} \},$$

where  $\mathcal{G} = \{h \leq \tau \leq n - h : (\tau - h, \tau + h] \cap \mathcal{T}^* = \emptyset\}$  is the collection of all feasible true null changepoints. Here,  $H_{0j}$  holds if and only if  $\hat{\tau}_j \in \mathcal{G}$ . The TUNE (Thresholding Universally and Nullifying change Effect) procedure introduced by [Jia et al. \(2024\)](#) rejects  $H_{0j}$  whenever a specified test statistic exceeds a universal threshold. TUNE is algorithm-agnostic, allowing the use of any changepoint estimation algorithms. It requires constructing localized two-sample statistics and determining an appropriate threshold by approximating the distribution of the maximum of these statistics under  $\Pr_{H_0}$ .

Interestingly, the ART methodology integrates naturally with TUNE. Concretely, for testing each  $H_{0j}$ , we use the statistic  $T_{n,\ell}$  on an interval  $\mathcal{I}_\ell = (\ell - h, \ell + h]$  and then define

$$\widehat{\mathcal{T}}_R = \{\widehat{\tau}_j \in \widehat{\mathcal{T}} : T_{n,\widehat{\tau}_j} > t_{\alpha,B}\}, \quad (3)$$

where  $t_{\alpha,B}$  is the threshold from Eq. (1).

**Theorem 5.** *With symmetric transformations, for any  $\alpha \in (0, 1)$ ,  $\text{FWER} \leq \alpha$ .*

Theorem 5 shows that the ART diagnostic achieves finite-sample FWER control, providing a model-agnostic and distribution-free enhancement of TUNE. Moreover, this integration remains algorithm-agnostic, as  $\widehat{\mathcal{T}}$  can be derived from any changepoint detection or localization algorithms. Notably, Theorem 5 mirrors Theorem 4 in spirit—both rely on pivotalness and distribution-freeness—despite targeting entirely different objectives. The proof follows directly from:

$$\begin{aligned} \text{FWER} &= \Pr \{ \text{there exists some } \widehat{\tau}_j \in \widehat{\mathcal{T}}_R \cap \mathcal{G} \}, \\ &\stackrel{(i)}{\leq} \Pr \left\{ \max_{\ell \in [L]; \widehat{\tau}_j \in \mathcal{G}} T_{n,\ell} > t_{\alpha,B} \right\} \\ &\stackrel{(ii)}{=} \Pr_{H_0} \left\{ \max_{\ell \in [L]; \widehat{\tau}_j \in \mathcal{G}} T_{n,\ell} > t_{\alpha,B} \right\} \stackrel{(iii)}{\leq} \Pr_{H_0} \left\{ \max_{\ell \in [L]} T_{n,\ell} > t_{\alpha,B} \right\} \stackrel{(iv)}{\leq} \alpha. \end{aligned}$$

Here, Setp (i) follows from the FWER definition and the rule given in (3); steps (ii)–(iv) mirror the arguments in Theorem 4, leveraging the pivotalness property from Theorem 2(ii) and distribution-freeness property from Corollary 1.

Table 1: Transformation, aggregation, and interval construction for ART.

Models	Transformation	Aggregation*	Result
Mean (Example1)	$K$ -means <sup>†</sup>	Rank CUSUM	Sections 4.1.1, 4.1.3
	$\mathbb{D}(z; \hat{f}_{\mathcal{D}}) = z$	Rank CUSUM	Sections 4.1.2, 4.2.1 (well-log data)
Regression (Example2)	$K$ -means	Rank CUSUM	Sections 4.1.1, 4.1.2
	$\mathbb{D}(z; \hat{f}_{\mathcal{D}}) = (y - x^{\top} \hat{\theta}_{\mathcal{D}})^{2\ddagger}$	Nonparametric likelihood	Section 4.1.1
Distribution	$\mathbb{D}(z; \hat{f}_{\mathcal{D}}) = -\phi(z)$	Nonparametric likelihood	Sections 4.1.1, 4.1.2
	Deep embedded clustering	Rank CUSUM	Section 4.2.2 (MNIST data)

<sup>†</sup> A standard  $K$ -means clustering approach is effective for low-dimensional data (see Algorithm S.1 in the supplementary material for details on centroid initialization and cluster number selection). In high-dimensional settings, it can be combined with screening methods (invariant to data order). For instance, in mean change scenarios, retain the dimensions corresponding to the top 10% of entries in  $|\hat{\theta}_{\mathcal{D},j}|$ ,  $j \in [d]$ , where  $\hat{\theta}_{\mathcal{D}} = n^{-1} \sum_{i=1}^n Z_i$  is the sample mean. In regression models, discard features for which  $\hat{\theta}_{\mathcal{D},j} = 0$ , where  $\hat{\theta}_{\mathcal{D}} \in \arg \min_{\theta} \{(2n)^{-1} \sum_{i=1}^n (y_i - x_i^{\top} \theta)^2 + \lambda_n \sum_{j=1}^d |\theta_j|\}$  is the global LASSO estimate with tuning parameter  $\lambda_n = 2\sqrt{(\log p)/n}$ . Subsequently, the standard  $K$ -means is applied to the remaining dimensions. Alternatively, screening and  $K$ -means may be performed jointly, as in the deep embedded clustering for high-dimensional data (see Algorithm S.2).

<sup>‡</sup>  $\hat{\theta}_{\mathcal{D}}$  is the global LASSO estimate as defined above.

\* Aggregation involves specifying a sequence of intervals  $\{\mathcal{I}_{\ell} : \ell \in [L]\}$ . For multiple changepoint testing, we use moving windows  $\{(\ell h - h, \ell h + h)\}_{\ell=1}^{\lfloor (n-h)/h \rfloor}$ . For localization with inference, we adopt seeded intervals (Kovács et al., 2023). For post-detection inference, we use  $\{(\ell - h, \ell + h)\}_{\ell=h}^{n-h}$ .

## 4 Numerical studies

We conduct numerical studies to evaluate the performance of the proposed ART method across several key tasks in changepoint detection: testing, localization with inference, and post-detection inference. Our experiments cover mean changes, shifts in regression coefficients, and more general distributional changes. Table 1 outlines the main implementation details for ART, highlighting model-assisted selections of transformation and aggregation choices, as well as multi-scale interval construction for each task. We set  $B = 200$  throughout, examining ART’s robustness to other  $B$  values in Section S.3.1 of the supplementary material.

## 4.1 Synthetic data

Let  $0_d \in \mathbb{R}^d$  denote the zero vector, omitting the subscript  $d$  when context is clear. Let  $I$  be the identity matrix. For a matrix  $(a_{ij}) \in \mathbb{R}^{d \times d}$ ,  $a_{ij}$  is its  $(i, j)$ -th element. The following models generate synthetic changes:

- Mean changes: Let  $\theta_1^* = 0$ , and define  $\theta_{k+1}^* - \theta_k^* = D_{k,s}$  for  $k \in [K^*]$ , where  $D_{k,s} \in \mathbb{R}^d$  has exactly  $s$  nonzero entries, each randomly set to  $c_\theta$  or  $-c_\theta$ , with the rest 0. Here,  $s$  indicates the number of components undergoing a change, and  $c_\theta$  specifies its magnitude. Noise is generated from  $P_\epsilon = P_{\epsilon,1}^d$ , where  $P_{\epsilon,1}$  is one of the following distributions: (i) Normal,  $c_P \cdot \mathcal{N}(0, 1)$ ; (ii)  $t(3)/c_P$ , a  $t$ -distribution with 3 degrees of freedom; or (iii) Log-normal,  $c_P \cdot \exp\{\mathcal{N}(0, 1)/10\}$ . The constant  $c_P$  calibrates the signal-to-noise ratio.
- Changes in regression coefficients: Let  $\theta_1^* = (0.5, 0, 0.5, 0_{d-3}^\top)^\top$ , and define  $\theta_{k+1}^* - \theta_k^* = D_{k,s}$  for  $k \in [K^*]$  using the same  $D_{k,s}$  construction. Covariates follow  $P_x = \mathcal{N}(0, (0.3^{|i-j|}))$ , with noise from  $P_{\epsilon,1}$  as in the mean change model.
- Distributional changes: We consider three patterns, each switching every two segments: (i) Covariance change:  $P_{2t-1}^* = \mathcal{N}(0, c_P \cdot I)$  and  $P_{2t}^* = \mathcal{N}(0, (0.9^{|i-j|}))$ ; (ii) Full change:  $P_{2t-1}^* = \mathcal{N}(0, I)$  and  $P_{2t}^* = \{t(3)\}^d$ ; and (iii) Partial change:  $P_{2t-1}^* = \mathcal{N}(0, I)$  and  $P_{2t}^* = \{t(3)\}^s \cdot \{\mathcal{N}(0, 1)\}^{d-s}$ , where  $s = \lfloor 0.4d \rfloor$ .

Each scenario is repeated 1,000 times. The subsequent subsections describe each task and its performance metrics.

### 4.1.1 Changepoint testing

We set the nominal Type-I error to  $\alpha = 0.1$  and assess empirical size and power.

Mean changes: We compare ART with two recently proposed high-dimensional mean change tests that aggregate component-wise CUSUM statistics. The first is the double-max-sum (DMS) test of [Wang and Feng \(2023\)](#), which relies on asymptotic theory. The second is the multiplier-bootstrap-based test of [Liu et al. \(2020\)](#) (LZZL).

Table 2: Empirical size and power of the ART, DMS, and LZZL tests for AMOC scenarios in mean change models under various error distributions.

Error	$(n,d)$	Null			Small change			Large change		
		ART	DMS	LZZL	ART	DMS	LZZL	ART	DMS	LZZL
Normal ( $c_P=0.25$ )	(100,100)	0.101	0.135	0.144	0.264	0.292	0.319	0.588	0.576	0.665
	(200,100)	0.096	0.117	0.133	0.481	0.525	0.542	0.826	0.941	0.955
	(300,100)	0.099	0.103	0.113	0.652	0.771	0.775	0.969	0.995	0.999
	(100,200)	0.095	0.134	0.152	0.205	0.225	0.299	0.531	0.488	0.593
	(200,200)	0.094	0.127	0.121	0.423	0.440	0.432	0.755	0.871	0.904
	(300,200)	0.098	0.111	0.096	0.619	0.654	0.664	0.874	0.989	0.997
$t$ ( $c_P=3$ )	(100,100)	0.098	0.053	0.051	0.141	0.157	0.164	0.455	0.484	0.520
	(200,100)	0.099	0.053	0.061	0.405	0.425	0.463	0.819	0.898	0.925
	(300,100)	0.100	0.058	0.052	0.603	0.675	0.708	0.908	0.988	0.993
	(100,200)	0.099	0.042	0.034	0.131	0.120	0.110	0.361	0.368	0.351
	(200,200)	0.093	0.048	0.055	0.392	0.360	0.321	0.772	0.836	0.843
	(300,200)	0.097	0.040	0.055	0.556	0.546	0.542	0.843	0.979	0.980
Log-normal ( $c_P=5$ )	(100,100)	0.097	0.136	0.127	0.220	0.311	0.338	0.483	0.658	0.690
	(200,100)	0.105	0.137	0.108	0.396	0.593	0.601	0.804	0.968	0.979
	(300,100)	0.099	0.129	0.105	0.683	0.814	0.836	0.931	0.999	1.000
	(100,200)	0.095	0.142	0.139	0.215	0.252	0.264	0.503	0.539	0.591
	(200,200)	0.101	0.142	0.135	0.437	0.493	0.484	0.793	0.937	0.950
	(300,200)	0.100	0.133	0.094	0.629	0.763	0.766	0.867	0.998	0.999

Initially, we consider AMOC scenarios where  $n \in \{100, 200, 300\}$  and  $d \in \{100, 200\}$ . Table 2 shows empirical size and power under various error distributions. Under the null ( $K^* = 0$ ), ART keeps size near the nominal level in all cases, while DMS and LZZL display mild over-rejection in smaller samples. Under the alternative, we place a single changepoint at  $\mathcal{T}^* = \lfloor 0.4n \rfloor$ , set  $s = 3$ , and consider small ( $c_\theta = 0.2$ ) and large ( $c_\theta = 0.3$ ) changes. The ART test achieves power comparable to DMS and LZZL, especially as  $n$  increases.

We also examine multiple changepoints for  $(n, d) = (200, 200)$ . Under the alternative, we set  $\mathcal{T}^* = \{\lfloor 0.3n \rfloor, \lfloor 0.4n \rfloor\}$  and  $s = 3$ . For ART, we employ window size  $h = 0.1n$  (see Table 1). Figure 2 illustrates empirical size and power across different error distributions. The ART

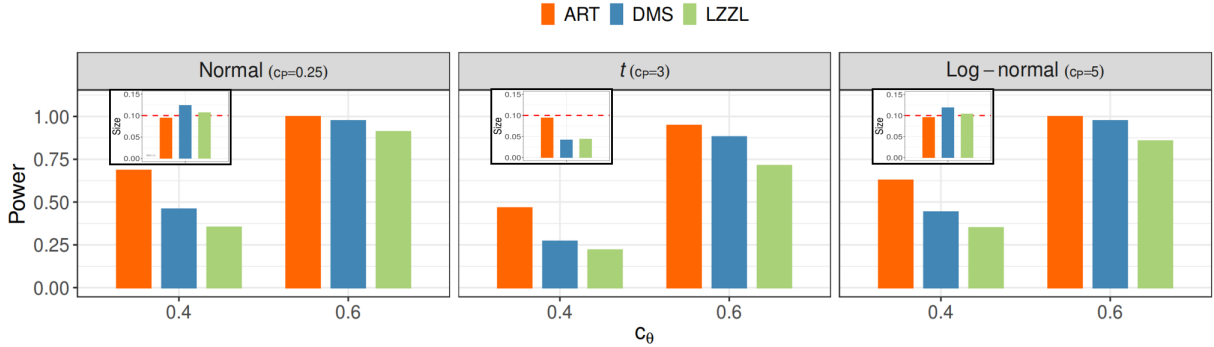


Figure 2: Empirical size and power of ART, DMS, and LZZL in mean change models with multiple changepoints under different error distributions. The red dashed line represents the nominal Type-I error.

test maintains size close to the nominal level and achieves the highest power, attributable to its multi-scale construction. In contrast, DMS and LZZL use single-scale approaches, which may miss signals if multiple changepoints are present.

Changes in regression coefficients: We compare ART with the bias-corrected quadratic-form-based CUSUM (QF-CUSUM) test proposed by [Zhao et al. \(2024\)](#), using their recommended tuning parameters.

We study AMOC scenarios with  $n \in \{100, 200, 400\}$  and  $d \in \{100, 200\}$ . Table 3 reports empirical size and power under different error settings. Under the null, ART upholds size at the nominal level for all sample sizes, irrespective of the employed transformation, while QF-CUSUM displays size inflation in smaller samples and appears conservative with log-normal errors. Under the alternative, we position a single changepoint at  $\mathcal{T}^* = \{\lfloor 0.4n \rfloor\}$ , set  $s = 5$ , and consider small ( $c_\theta = 0.5$ ) or large ( $c_\theta = 0.7$ ) changes. The ART test is comparable to QF-CUSUM overall and outperforms it under log-normal errors for small changes. Notably, QF-CUSUM requires ( $O(n)$ ) LASSO fits, bias correction, and suitable randomization, whereas ART with a deviance transformation only needs one global LASSO fit, followed by ranking and aggregation. Despite its simplicity, ART maintains valid size and competitive power.

Distributional changes: We compare ART with two nonparametric changepoint detection methods: ecp (energy-based) ([Matteson and James, 2014](#)) and changeforest (random-forest-

Table 3: Empirical size and power of the ART and QF-CUSUM (QF) tests for AMOC scenarios in regression models under different error distributions. ART with clustering and deviance transformations is labeled ART.cl and ART.de, respectively.

Error	$(n, d)$	Null			Small change			Large change		
		ART.cl	ART.de	QF	ART.cl	ART.de	QF	ART.cl	ART.de	QF
Normal ( $c_P=0.25$ )	(100,100)	0.098	0.105	0.225	0.736	0.705	0.769	0.832	0.970	0.995
	(200,100)	0.092	0.097	0.064	0.830	0.928	0.933	0.898	0.999	1.000
	(400,100)	0.102	0.099	0.050	0.908	0.999	0.996	0.913	1.000	1.000
	(100,200)	0.098	0.093	0.192	0.656	0.716	0.760	0.765	0.962	0.990
	(200,200)	0.095	0.098	0.056	0.791	0.916	0.799	0.877	0.997	0.999
	(400,200)	0.096	0.105	0.033	0.893	0.997	0.955	0.899	1.000	1.000
$t$ ( $c_P=3$ )	(100,100)	0.105	0.095	0.292	0.520	0.519	0.781	0.622	0.835	0.974
	(200,100)	0.101	0.099	0.136	0.669	0.783	0.764	0.801	0.991	0.990
	(400,100)	0.101	0.092	0.075	0.762	0.976	0.985	0.877	1.000	1.000
	(100,200)	0.100	0.101	0.299	0.423	0.509	0.724	0.580	0.818	0.960
	(200,200)	0.087	0.102	0.095	0.625	0.773	0.715	0.795	0.985	0.973
	(400,200)	0.115	0.099	0.073	0.759	0.971	0.935	0.874	1.000	1.000
Log-normal ( $c_P=5$ )	(100,100)	0.093	0.099	0.083	0.494	0.449	0.317	0.615	0.825	0.903
	(200,100)	0.098	0.102	0.007	0.630	0.714	0.393	0.826	0.989	0.989
	(400,100)	0.098	0.102	0.002	0.754	0.940	0.546	0.887	1.000	1.000
	(100,200)	0.095	0.094	0.083	0.418	0.466	0.246	0.588	0.820	0.877
	(200,200)	0.097	0.094	0.009	0.607	0.692	0.271	0.778	0.983	0.954
	(400,200)	0.093	0.104	0.001	0.752	0.933	0.288	0.876	1.000	0.997

based) (Londschieen et al., 2023). Both ecp and changeforest rely on permutation or pseudo-permutation for significance testing.

We restrict attention to AMOC scenarios with  $n \in \{50, 100, 200\}$  and  $d \in \{5, 10\}$ . Table 4 lists empirical size and power for three types of distributional changes. Under the null, ART and ecp maintain size near the nominal level, while changeforest tends to over-reject. Under the alternative (with  $\mathcal{T}^* = \{\lfloor 0.5n \rfloor\}$ ), ecp struggles to detect covariance or partial changes, and changeforest attains higher power (but with inflated size). In contrast, ART offers stable size control and robust power across the different scenarios.



Table 4: Empirical size and power of the ART, ecp, and changeforest (CF) tests for AMOC scenarios under distributional changes ( $c_P = 1$ ).

$(n, d)$	Null			Covariance change			Full change			Partial change		
	ART	ecp	CF	ART	ecp	CF	ART	ecp	CF	ART	ecp	CF
(50,5)	0.104	0.110	0.157	0.442	0.262	0.917	0.905	0.535	0.982	0.343	0.112	0.802
(100,5)	0.099	0.093	0.131	0.735	0.310	1.000	1.000	0.932	1.000	0.558	0.125	0.985
(200,5)	0.103	0.097	0.130	0.989	0.517	1.000	1.000	1.000	1.000	0.896	0.135	1.000
(50,10)	0.097	0.101	0.149	0.455	0.320	0.990	1.000	0.572	0.999	0.526	0.113	0.947
(100,10)	0.099	0.097	0.135	0.862	0.329	1.000	1.000	0.980	1.000	0.874	0.170	1.000
(200,10)	0.104	0.100	0.141	1.000	0.502	1.000	1.000	1.000	1.000	0.992	0.198	1.000

#### 4.1.2 Changepoint localization with inference

We compare the ART localization method with NSP (Fryzlewicz, 2024a) and its robust variant RNSP (Fryzlewicz, 2024b), which detects changes in the median (equal to the mean under symmetric errors). Both NSP and RNSP necessitate setting the number of intervals  $M$  over which an estimation procedure is iteratively applied. Following Fryzlewicz (2024a), we set  $M = 1,000$ . For ART, we use seeded intervals (Kovács et al., 2023) with sets of  $\{381, 579, 778\}$  intervals for  $n \in \{200, 300, 400\}$  respectively. We track several measures:

- P (positive): number of localized intervals;
- TP (true positive): number of intervals containing at least one changepoint;
- TPP (true positive proportion): TP/P;
- AveLen: average length of intervals deemed true positives;
- Hausdorff distance:  $d_H = \max \left\{ \max_{k \in [K^*]} \min_{\hat{\tau} \in \hat{\mathcal{T}}} |\tau_k^* - \hat{\tau}|, \max_{\hat{\tau} \in \hat{\mathcal{T}}} \min_{k \in [K^*]} |\tau_k^* - \hat{\tau}| \right\}$ , which assesses localization accuracy.

Both ART and (R)NSP aim to control the probability of localizing intervals that do not contain actual changepoints, thereby controlling  $\text{FWER} = \Pr\{P - TP > 0\}$  at a nominal significance level  $\alpha = 0.1$ .

Table 5: Comparisons of ART, NSP, and RNSP for changepoint localization with inference across different models and data distributions. The symbol “-” indicates scenarios where entries are not applicable.

Model ( $n,d$ )	$Error$ ( $c_\theta, c_P$ )	Method	FWER	P	TP	TPP	AveLen	$d_H$	Time (s)
Mean (300,1)	Normal (1,1)	ART	0.063	1.941	1.878	0.975	42.855	15.005	3.202
		NSP	0.067	1.991	1.908	0.973	46.492	20.553	1.439
		RNSP	0.002	1.664	1.662	0.999	61.525	37.157	8.841
	Normal (2,1)	ART	0.051	2.043	1.990	0.981	25.967	3.624	3.289
		NSP	0.065	2.085	1.999	0.975	15.337	7.207	1.239
		RNSP	0.001	2.001	2.000	1.000	34.765	4.652	7.905
	$t$ (1, $\sqrt{3}$ )	ART	0.055	2.045	1.990	0.981	34.622	5.488	3.287
		NSP	0.993	8.291	1.712	0.240	19.978	78.799	1.126
		RNSP	0.000	1.997	1.997	1.000	47.179	8.332	7.568
	$t$ (2, $\sqrt{3}$ )	ART	0.060	2.058	1.996	0.979	24.418	3.878	3.271
		NSP	0.985	8.708	1.967	0.267	8.717	78.034	1.066
		RNSP	0.002	2.002	2.000	1.000	29.993	2.544	7.375
Regression (200,5)		ART	0.066	1.860	1.793	0.971	37.874	14.731	3.343
		NSP	0.000	1.897	1.897	1.000	36.790	15.331	26.046
Regression (400,5)		ART	0.084	2.063	1.976	0.968	44.901	8.778	6.437
		NSP	0.000	1.999	1.999	1.000	40.779	12.623	35.913
Regression (200,10)	Normal (2,1)	ART	0.051	1.820	1.767	0.977	39.735	16.861	4.217
		NSP	0.000	1.597	1.597	1.000	55.829	29.898	38.048
Regression (400,10)		ART	0.082	2.071	1.983	0.969	46.939	8.886	7.347
		NSP	0.000	1.980	1.980	1.000	65.960	18.781	48.552
Regression (200,400)		ART	0.066	1.404	1.338	0.945	51.168	39.311	6.869
		NSP	-	-	-	-	-	-	-
Regression (400,400)		ART	0.068	2.029	1.958	0.972	49.920	10.538	11.171
		NSP	-	-	-	-	-	-	-
Distribution (300,30)	Covariance change (-,0.25)	ART	0.054	2.057	1.999	0.981	22.437	4.114	3.581
		(R)NSP	-	-	-	-	-	-	-
	Full change (-,0.25)	ART	0.055	2.047	1.995	0.983	23.541	4.512	3.565
		(R)NSP	-	-	-	-	-	-	-
	Partial change (-,0.25)	ART	0.045	1.971	1.922	0.980	62.517	12.191	3.571
		(R)NSP	-	-	-	-	-	-	-

The underlying changepoint model has two changepoints at  $\mathcal{T}^* = \{\lfloor 0.3n \rfloor, \lfloor 0.6n \rfloor\}$  in univariate mean change scenarios, regression coefficient changes ( $d \in \{5, 10, 400\}$ ,  $s = 5$ ), and distributional changes ( $d = 30$ ). Note that NSP does not apply to high-dimensional regression or distributional changes, and RNSP is limited to univariate median changes. Table 5 summarizes the simulation outcomes for ART, NSP, and RNSP under different models and data distributions. As expected, ART controls the FWER below the nominal significance level across all settings, while delivering high TPP, short AveLen, and accurate localization. By contrast:

- In univariate mean change settings, NSP controls the FWER under normal errors but exhibits severe inflation under  $t$ -distributed noises. It generally produces shorter intervals (especially for large changes  $c_\theta = 2$ ), yet reports more false positives in heavy-tailed settings. RNSP addresses false positives but is more conservative, possibly yielding longer intervals and reduced localization accuracy.
- For regression coefficient changes under normal errors, NSP slightly surpasses ART in TPP and interval lengths when  $d$  is small, but intervals widen at higher dimensions.

Additionally, ART performs only one global score transformation, then computes multi-scale statistics  $T_{n,\ell}$  from local ranks. In contrast, (R)NSP often necessitates repeated multisolution sup-norm loss minimizations (Fryzlewicz, 2024a,b) over a large collection of intervals, increasing computational burden (see Table 5), particularly under complex models.

### 4.1.3 Post-detection inference

We examine mean change models with  $n = 600$ ,  $d \in \{10, 200\}$ ,  $K^* = 3$ , and  $\mathcal{T}^* = \{\lfloor kn/(K^* + 1) \rfloor, k = 1, \dots, K^*\}$ , setting  $s = 3$ . We apply the Inspect procedure (Wang and Samworth, 2018) to detect changepoints, obtaining  $\widehat{\mathcal{T}}$ . To validate these detections via the multiple testing framework (2) (with  $h = 30$ ), we use the proposed ART diagnostic and TUNE (Jia et al., 2024). Following Jia et al. (2024), TUNE is implemented in two ways: (i) a Wald-type statistic with asymptotic thresholds; and (ii) an  $\ell_\infty$ -aggregation-based statistic with bootstrap-calibrated thresholds. For ART, we employ a window size  $h = 30$ . Each method

is evaluated on two metrics: FWER and power, where

$$\text{Power} = \mathbb{E} \left[ \frac{\left| \left\{ \hat{\tau}_j \in \hat{\mathcal{T}} : \hat{\tau}_j \in \hat{\mathcal{T}}_R, \hat{\tau}_j \notin \mathcal{G} \right\} \right|}{\left| \left\{ \hat{\tau}_j \in \hat{\mathcal{T}} : \hat{\tau}_j \notin \mathcal{G} \right\} \right|} \right],$$

reflecting the expected fraction of detected changepoints deemed reliable. The nominal significance level is set to  $\alpha = 0.1$ .

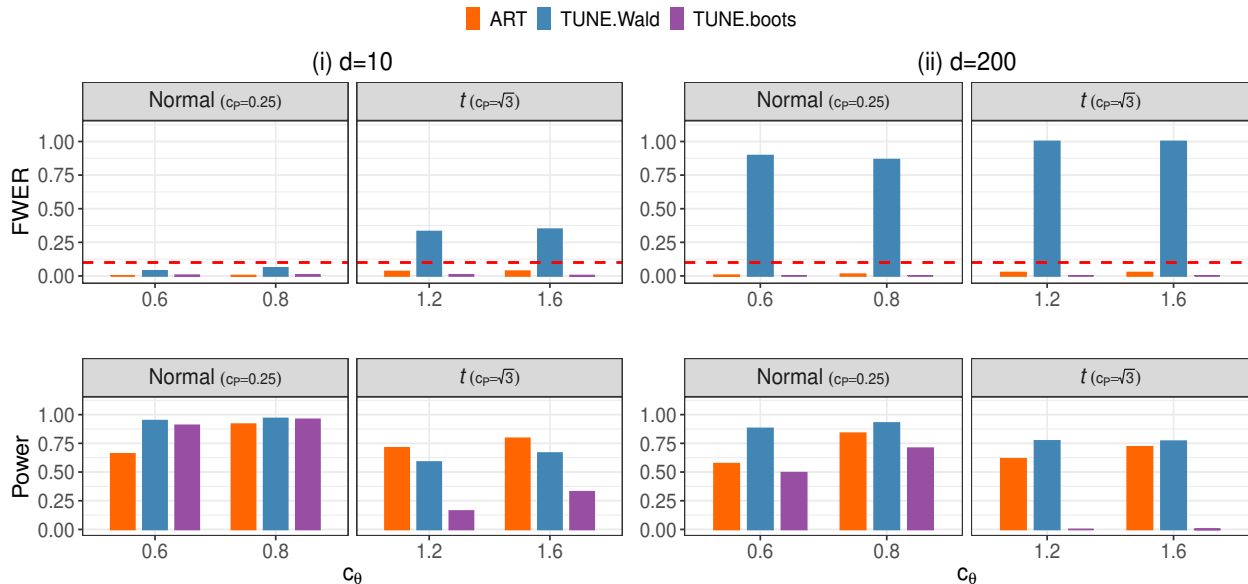


Figure 3: Comparisons of ART and TUNE (TUNE.Wald for (i) and TUNE.boots for (ii)) for post-detection inference under various error settings. The red dashed line represents the nominal FWER level.

Figure 3 compares ART and TUNE across different model dimensions and error distributions. In every setting, ART keeps the FWER below the nominal level and achieves high power. By contrast, TUNE with Wald thresholds performs well for low-dimensional normal data but inflates FWER in other contexts, suggesting a breakdown of asymptotic approximations. TUNE with bootstrap thresholds preserves valid FWER but is conservative for  $t$ -distributed errors. These results confirm the distribution-free and model-agnostic benefits of ART in post-detection inference.

## 4.2 Real-data analysis

### 4.2.1 Well-log dataset

We apply the ART localization procedure to detect changepoints in a well-log dataset (Ruanaidh and Fitzgerald, 1996), which contains  $n = 4,050$  depth-indexed nuclear magnetic measurements recorded along a borehole. These measurements are commonly assumed to be piecewise constant (Fearnhead and Rigall, 2019), with changepoints indicating geological transitions such as shifts in rock type. Identifying these boundaries informs lithological structure characterization and supports more effective exploration and production decisions.

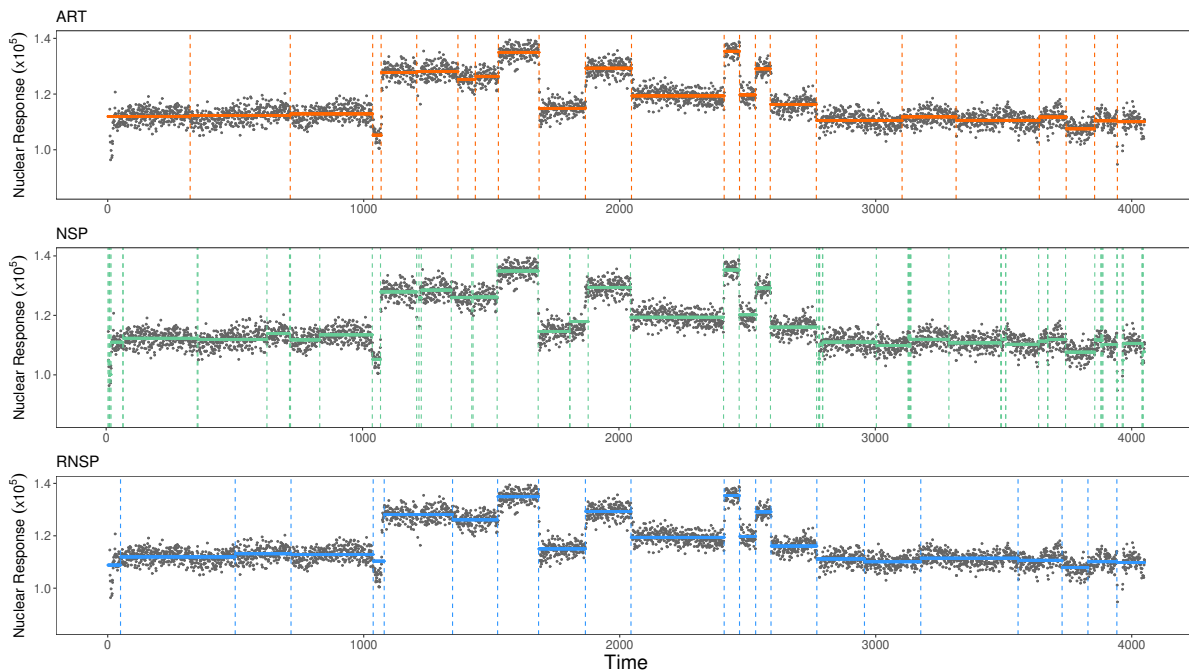


Figure 4: The gray dots show the well-log measurements, while the vertical lines mark the detected changepoints at  $\alpha = 0.1$ . The horizontal lines display the median within each segment.

ART follows the guidelines in Table 1, using 3,216 seeded intervals. As benchmarks, we employ NSP and RNSP with  $M = 3,200$ . The nominal significance level is  $\alpha = 0.1$ . ART, NSP, and RNSP detect 23, 43, and 20 changepoints, respectively, with running times (in minutes) 1.106, 5.989, and 2.350. Figure 4 presents the data points alongside each method’s detected changepoints. NSP appears to overfit because its least-squares-based minimization

is sensitive to outliers, producing isolated changepoints. RNSP and ART produce similar, more robust detection results.

#### 4.2.2 MNIST dataset

In this study, we examine the performance of the proposed ART method on the high-dimensional, non-Euclidean MNIST dataset (LeCun et al., 1998), which comprises 70,000 grayscale images of handwritten digits (0-9), each of size  $28 \times 28$  pixels. We construct four distinct scenarios (see Figure 5) for changepoint detection in sequences of these images: (i) a control setting with  $n$  samples exclusively of digit “0”, containing no changepoints; (ii) a small-signal scenario (3-8-3) where 40% of the samples are digit “3”, followed by 20% digit “8”, and then 40% digit “3” again, reflecting subtle changes due to the visual similarity between “3” and “8”; (iii) a multiple changepoint scenario (1-2-3), comprising 40% digit “1”, 20% digit “2”, and 40% digit “3”; and (iv) a multiple changepoint setting (0-5), with  $n$  samples evenly distributed across digits “0” to “5”. In Scenarios (i)–(iii), we set  $n = 150$ ; for Scenario (iv),  $n = 600$ . All pixel values are normalized to  $[0, 1]$ . We consider a sequence of tasks—namely, changepoint testing, localization with inference, and post-detection inference—across the four scenarios. ART is implemented as described in Table 1, employing a transformation based on deep embedded clustering (Xie et al., 2016), followed by rank CUSUM aggregation. We fix the nominal significance level to  $\alpha = 0.1$  throughout.

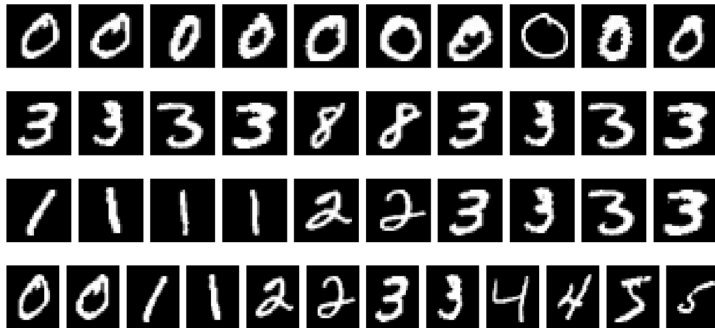


Figure 5: Illustration of the four changepoint detection scenarios using the MNIST dataset.

**Changepoint testing:** We use changeforest (Londschien et al., 2021) as a benchmark

for changepoint testing; see Section 3.1. For ART, we employ moving windows with  $h = 30$ . Figure 6 shows that, in the control scenario (0), both approaches yield similarly high p-values, confirming the absence of changepoints. In the small-signal scenario (3-8-3), changeforest fails to detect changepoints (producing a p-value of approximately 0.905), whereas ART obtains a p-value below 0.01, successfully signaling changes. In the multiple changepoint scenarios (1-2-3 and 0-5), both methods effectively detect changepoints.

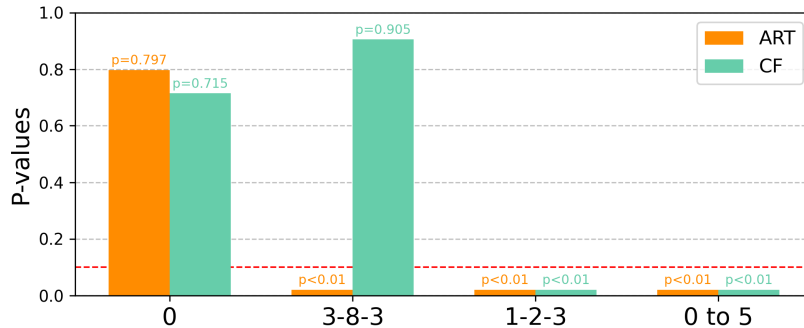


Figure 6: Comparison of p-values from the ART and changeforest (CF) methods across different MNIST scenarios. The red dashed line indicates the nominal level.

**Changepoint localization with inference:** After rejecting the null hypothesis in Scenarios (ii)–(iv), we apply the ART localization procedure to identify changepoints. We select multi-scale intervals comprising all subintervals of  $(0, n]$ . Table 6 summarizes the localization results, demonstrating that ART accurately identifies regions containing true changepoints.

Table 6: Localization results for the ART method on the MNIST dataset under various changepoint scenarios.

Scenario	$K^*$	P	TP	TPP	AveLen	$d_H$
3-8-3	2	2	2	1	32	11
1-2-3	2	2	2	1	18	2
0-5	5	5	5	1	31.2	13

**Post-detection inference:** We note that the ART localization procedure already provides reliable changepoint estimates, evidenced by the small Hausdorff distance ( $d_H$ ) in Ta-

ble 6. Moreover, ART can refine detection results from other methods via post-selection inference. Specifically, we consider the multiple testing framework (2) with  $h = 20$ , where changepoints are estimated using changeforest and Inspect. The default Inspect implementation often yields redundant, locally clustered changepoints, so we apply a screening procedure: We select the changepoint with the largest CUSUM value, remove any points within  $\pm 20$  of that location, and repeat until no candidate remains. For ART, we use multi-scale intervals defined by moving windows of size  $h$ . We track several metrics: P (positive) denotes the number of estimated changepoints or retained changepoints after post-detection inference; TP (true positive) is the number of true changepoints among them; and TPP (true positive proportion) is  $TP/P$ . Table 7 shows that both changeforest and Inspect alone tend to overestimate (leading to large P and  $d_H$ ), despite correctly including all true changepoints ( $TP = K^*$ ). Refining these estimates with ART removes false positives, achieving perfect TPP and minimal Hausdorff distance. Hence, ART serves as an effective and reliable tool for post-detection inference.

Table 7: Post-detection inference results for the ART method compared to changeforest and Inspect on the MNIST dataset.

Scenario	Method	$K^*$	P	TP	TPP	$d_H$
3-8-3	Inspect	2	4	2	0.5	31
	Inspect+ART	2	2	2	1	0
1-2-3	CF	2	2	2	1	0
	CF+ART	2	2	2	1	0
	Inspect	2	4	2	0.5	26
	Inspect+ART	2	2	2	1	0
0-5	CF	5	8	5	0.625	343
	CF+ART	5	5	5	1	0
	Inspect	5	17	5	0.294	350
	Inspect+ART	5	5	5	1	1



## 5 Conclusion

This paper introduces a distribution-free, model-agnostic approach to changepoint detection that guarantees finite-sample error control. By leveraging symmetric transformations and rank-based aggregations, the proposed framework broadens the applicability of existing methods, offering reliable performance in the absence of stringent distributional or model assumptions. Numerical studies demonstrate that even simple transformations, such as global model fits or naive reference models, can achieve performance comparable to more complex, model-specific approaches. This highlights the practicality of our approach, providing a flexible and robust solution for changepoint detection in complex and less-structured data.

Several avenues for future research remain. First, it would be valuable to explore methods for selecting or constructing optimal or informative score transformations. Additionally, investigating how multiple scores can be efficiently combined to further enhance detection power would be a promising direction. Second, the concept of *pivotalness to changes* provides a novel framework for distribution-free inference in non-exchangeable data settings. This concept may offer new theoretical insights and can potentially be extended to other areas of statistical inference. Finally, extending the proposed framework to online or streaming data scenarios presents a natural and exciting challenge.

## Supplementary material

The supplementary material contains all the theoretical proofs, along with additional algorithmic and numerical details.

## References

- Angelopoulos, A. N., Barber, R. F., and Bates, S. (2024), “Theoretical foundations of conformal prediction,” *arXiv preprint arXiv:2411.11824*.
- Antoch, J. and Hušková, M. (2001), “Permutation tests in change point analysis,” *Statistics & Probability Letters*, 53, 37–46.
- Arlot, S., Celisse, A., and Harchaoui, Z. (2019), “A kernel multiple change-point algorithm via model selection,” *Journal of Machine Learning Research*, 20, 1–56.

- Arthur, D. and Vassilvitskii, S. (2007), “ $K$ -means++: The advantages of careful seeding,” *ACM-SIAM Symposium on Discrete Algorithms*, 1027–1035.
- Bai, J. (2010), “Common breaks in means and variances for panel data,” *Journal of Econometrics*, 157, 78–92.
- Baranowski, R., Chen, Y., and Fryzlewicz, P. (2019), “Narrowest-over-threshold detection of multiple change points and change-point-like features,” *Journal of the Royal Statistical Society: Series B (Statistical Methodology)*, 81, 649–672.
- Carrington, R. and Fearnhead, P. (2025), “Improving power by conditioning on less in post-selection inference for changepoints,” *Statistics and Computing*, 35, 1–23.
- Chan, H. P. and Walther, G. (2013), “Detection with the scan and the average likelihood ratio,” *Statistica Sinica*, 23, 409–428.
- Chen, H. and Chu, L. (2023), “Graph-based change-point analysis,” *Annual Review of Statistics and its Application*, 10, 475–499.
- Chen, H., Ren, H., Yao, F., and Zou, C. (2023), “Data-driven selection of the number of change-points via error rate control,” *Journal of the American Statistical Association*, 118, 1415–1428.
- Chen, H. and Zhang, N. (2015), “Graph-based change-point detection,” *The Annals of Statistics*, 43, 139–176.
- Cho, H. and Fryzlewicz, P. (2015), “Multiple-change-point detection for high dimensional time series via sparsified binary segmentation,” *Journal of the Royal Statistical Society: Series B (Statistical Methodology)*, 77, 475–507.
- Cléménçon, S., Limnios, M., and Vayatis, N. (2021), “Concentration inequalities for two-sample rank processes with application to bipartite ranking,” *Electronic Journal of Statistics*, 15, 4659–4717.
- Csörgö, M. and Horváth, L. (1997), *Limit theorems in change-point analysis*, Wiley Series in Probability and Statistics, Wiley.
- Darkhovskh, B. (1976), “A nonparametric method for the a posteriori detection of the “disorder” time of a sequence of independent random variables,” *Theory of Probability & Its Applications*, 21, 178–183.
- Duy, V. N. L., Toda, H., Sugiyama, R., and Takeuchi, I. (2020), “Computing valid p-value for optimal changepoint by selective inference using dynamic programming,” *Advances in Neural Information Processing Systems*, 33, 11356–11367.
- Eichinger, B. and Kirch, C. (2018), “A MOSUM procedure for the estimation of multiple random change points,” *Bernoulli*, 24, 526–564.
- Einmahl, J. H. J. and McKeague, I. W. (2003), “Empirical likelihood based hypothesis testing,” *Bernoulli*, 9, 267–290.
- Fang, X., Li, J., and Siegmund, D. (2020), “Segmentation and estimation of change-point models: false positive control and confidence regions,” *The Annals of Statistics*, 48, 1615–1647.
- Fearnhead, P. and Rigail, G. (2019), “Changepoint detection in the presence of outliers,” *Journal of the American Statistical Association*, 114, 169–183.
- Frick, K., Munk, A., and Sieling, H. (2014), “Multiscale change point inference,” *Journal of the Royal Statistical Society: Series B (Statistical Methodology)*, 76, 495–580.

- Fryzlewicz, P. (2014), “Wild binary segmentation for multiple change-point detection,” *The Annals of Statistics*, 42, 2243–2281.
- (2024a), “Narrowest significance pursuit: inference for multiple change-points in linear models,” *Journal of the American Statistical Association*, 119, 1633–1646.
- (2024b), “Robust narrowest significance pursuit: Inference for multiple change-points in the median,” *Journal of Business & Economic Statistics*, 1–14.
- Hao, N., Niu, Y. S., and Zhang, H. (2013), “Multiple change-point detection via a screening and ranking algorithm,” *Statistica Sinica*, 23, 1553–1572.
- Hemerik, J. and Goeman, J. (2018), “Exact testing with random permutations,” *Test*, 27, 811–825.
- Hušková, M. (1997), “Limit theorems for rank statistics,” *Statistics & Probability Letters*, 32, 45–55.
- Hyun, S., G’Sell, M., and Tibshirani, R. J. (2018), “Exact post-selection inference for the generalized lasso path,” *Electronic Journal of Statistics*, 12, 1053–1097.
- Hyun, S., Lin, K. Z., G’Sell, M., and Tibshirani, R. J. (2021), “Post-selection inference for change-point detection algorithms with application to copy number variation data,” *Biometrics*, 77, 1037–1049.
- Jewell, S., Fearnhead, P., and Witten, D. (2022), “Testing for a change in mean after changepoint detection,” *Journal of the Royal Statistical Society: Series B (Statistical Methodology)*, 84, 1082–1104.
- Jia, Y., Liu, J., Wang, G., Wang, Z., and Zou, C. (2024), “TUNE: Algorithm-Agnostic Inference after Changepoint Detection,” *arXiv preprint arXiv:2409.15676*.
- Jirak, M. (2015), “Uniform change point tests in high dimension,” *The Annals of Statistics*, 43, 2451–2483.
- Kaul, A., Jandhyala, V. K., and Fotopoulos, S. B. (2019), “An efficient two step algorithm for high dimensional change point regression models without grid search,” *Journal of Machine Learning Research*, 20, 1–40.
- Killick, R., Fearnhead, P., and Eckley, I. A. (2012), “Optimal detection of changepoints with a linear computational cost,” *Journal of the American Statistical Association*, 107, 1590–1598.
- Kovács, S., Bühlmann, P., Li, H., and Munk, A. (2023), “Seeded binary segmentation: a general methodology for fast and optimal changepoint detection,” *Biometrika*, 110, 249–256.
- LeCun, Y., Bottou, L., Bengio, Y., and Haffner, P. (1998), “Gradient-based learning applied to document recognition,” *Proceedings of the IEEE*, 86, 2278–2324.
- Lee, S., Seo, M. H., and Shin, Y. (2016), “The lasso for high dimensional regression with a possible change point,” *Journal of the Royal Statistical Society: Series B (Statistical Methodology)*, 78, 193–210.
- Lehmann, E. L. and D’Abrera, H. J. (1975), *Nonparametrics: statistical methods based on ranks.*, Holden-day.
- Lehmann, E. L. and Romano, J. P. (2021), *Testing statistical hypotheses*, Springer, Cham.
- Lei, J., G’Sell, M., Rinaldo, A., Tibshirani, R. J., and Wasserman, L. (2018), “Distribution-free predictive inference for regression,” *Journal of the American Statistical Association*, 113, 1094–1111.

- Leonardi, F. and Bühlmann, P. (2016), “Computationally efficient change point detection for high-dimensional regression,” *arXiv preprint arXiv:1601.03704*.
- Li, J., Fearnhead, P., Fryzlewicz, P., and Wang, T. (2024), “Automatic change-point detection in time series via deep learning,” *Journal of the Royal Statistical Society: Series B (Statistical Methodology)*, 86, 273–285.
- Liu, B., Zhou, C., Zhang, X., and Liu, Y. (2020), “A unified data-adaptive framework for high dimensional change point detection,” *Journal of the Royal Statistical Society: Series B (Statistical Methodology)*, 82, 933–963.
- Lombard, F. (1987), “Rank tests for changepoint problems,” *Biometrika*, 74, 615–624.
- Lonschien, M., Bühlmann, P., and Kovács, S. (2023), “Random forests for change point detection,” *Journal of Machine Learning Research*, 24, 1–45.
- Lonschien, M., Kovács, S., and Bühlmann, P. (2021), “Change-point detection for graphical models in the presence of missing values,” *Journal of Computational and Graphical Statistics*, 30, 768–779.
- Lung-Yut-Fong, A., Lévy-Leduc, C., and Cappé, O. (2015), “Homogeneity and change-point detection tests for multivariate data using rank statistics,” *Journal de la société française de statistique*, 156, 133–162.
- Madrid Padilla, O. H., Yu, Y., Wang, D., and Rinaldo, A. (2021), “Optimal nonparametric change point analysis,” *Electronic Journal of Statistics*, 15, 1154–1201.
- Matteson, D. S. and James, N. A. (2014), “A nonparametric approach for multiple change point analysis of multivariate data,” *Journal of the American Statistical Association*, 109, 334–345.
- Niu, Y. S. and Zhang, H. (2012), “The screening and ranking algorithm to detect DNA copy number variations,” *The Annals of Applied Statistics*, 6, 1306.
- Pettitt, A. N. (1979), “A non-parametric approach to the change-point problem,” *Journal of the Royal Statistical Society: Series C (Applied Statistics)*, 28, 126–135.
- Ruanaidh, J. J. Ó. and Fitzgerald, W. J. (1996), *Numerical Bayesian methods applied to signal processing*, Springer New York.
- Tibshirani, R., Walther, G., and Hastie, T. (2001), “Estimating the number of clusters in a data set via the gap statistic,” *Journal of the Royal Statistical Society: Series B (Statistical Methodology)*, 63, 411–423.
- Truong, C., Oudre, L., and Vayatis, N. (2020), “Selective review of offline change point detection methods,” *Signal Processing*, 167, 107299.
- van der Vaart, A. W. and Wellner, J. A. (1996), *Weak convergence and empirical processes*, New York: Springer.
- Vapnik, V. N. (1998), *Statistical learning theory*, Wiley New York.
- Vovk, V., Gammerman, A., and Shafer, G. (2005), *Algorithmic learning in a random world*, vol. 29, Springer.
- Vovk, V., Nouretdinov, I., and Gammerman, A. (2003), “Testing exchangeability on-line,” *International Conference on Machine Learning*, 20, 768–775.

- Wang, D., Zhao, Z., Lin, K. Z., and Willett, R. (2021), “Statistically and computationally efficient change point localization in regression settings,” *Journal of Machine Learning Research*, 22, 11255–11300.
- Wang, G. and Feng, L. (2023), “Computationally efficient and data-adaptive changepoint inference in high dimension,” *Journal of the Royal Statistical Society: Series B (Statistical Methodology)*, 85, 936–958.
- Wang, G., Zou, C., and Yin, G. (2018), “Change-point detection in multinomial data with a large number of categories,” *The Annals of Statistics*, 46, 2020–2044.
- Wang, T. and Samworth, R. J. (2018), “High dimensional change point estimation via sparse projection,” *Journal of the Royal Statistical Society: Series B (Statistical Methodology)*, 80, 57–83.
- Xie, J., Girshick, R., and Farhadi, A. (2016), “Unsupervised deep embedding for clustering analysis,” *International Conference on Machine Learning*, 48, 478–487.
- Xu, H., Wang, D., Zhao, Z., and Yu, Y. (2024), “Change-point inference in high-dimensional regression models under temporal dependence,” *The Annals of Statistics*, 52, 999–1026.
- Yu, M. and Chen, X. (2021), “Finite sample change point inference and identification for high-dimensional mean vectors,” *Journal of the Royal Statistical Society: Series B (Statistical Methodology)*, 83, 247–270.
- (2022), “A robust bootstrap change point test for high-dimensional location parameter,” *Electronic Journal of Statistics*, 16, 1096–1152.
- Zhang, J. (2006), “Powerful two-sample tests based on the likelihood ratio,” *Technometrics*, 48, 95–103.
- Zhang, Y., Wang, R., and Shao, X. (2022), “Adaptive inference for change points in high-dimensional data,” *Journal of the American Statistical Association*, 117, 1751–1762.
- Zhao, Z., Luo, X., Liu, Z., and Wang, D. (2024), “Optimal change-point testing for high-dimensional linear models with temporal dependence,” *arXiv preprint arXiv:2205.03880*.
- Zou, C., Yin, G., Feng, L., and Wang, Z. (2014), “Nonparametric maximum likelihood approach to multiple change-point problems,” *The Annals of Statistics*, 42, 970–1002.

# Supplementary material for “ART: Distribution-free and model-agnostic changepoint detection with finite-sample guarantees”

The supplementary material contains all the theoretical proofs, along with additional algorithmic and numerical details. Section S.1 presents implementation details of clustering transformations, including a  $K$ -means clustering procedure for parametric models (Section S.1.1) and a deep embedded clustering approach for high-dimensional data (Section S.1.2). Section S.2 collects proofs of Theorems 1–3, Corollary 1, and Proposition 1. Section S.3 shows additional simulation results, including the impact of parameter  $B$  in the ART method, a comparison between deviance and clustering transformations, and evidence of ART’s robustness under departures from data independence.

## S.1 Clustering transformations

### S.1.1 $K$ -means clustering for parametric models

Algorithm S.1 presents a  $K$ -means clustering-based transformation for constructing scores in parametric models. The algorithm alternates between assigning group memberships and estimating model parameters until convergence.

**Remark 1** (On the loss function). *Choose loss function  $\rho(z, f)$  to suit the specific problem. For instance, in mean estimation, set  $\rho(z, f) = \|z - f\|_2^2$ , while for regression, use  $\rho(z, f) = (y - x^\top f)^2$ .*

**Remark 2** (On initial cluster centroids). *For mean models, we use a  $K$ -means++ initialization (Arthur and Vassilvitskii, 2007) with a minor modification to ensure a symmetric transformation. Let  $D(z)$  be the shortest distance from a point  $z$  to the closest centroid already chosen. First, set  $f_1^{(0)} = n^{-1} \sum_{i=1}^n Z_i$ . Next, select the subsequent centroid as the data point achieving the largest  $D(z)$ . Repeat until a total of  $K$  centroids are obtained.*

*For regression models with  $Z_i = (y_i, x_i)$ , we first apply this modified  $K$ -means++ procedure to  $\{\tilde{z}_i = y_i x_i\}_{i=1}^n$ , yielding preliminary centroids. Then perform Step 1 of Algorithm S.1 with*

---

**Algorithm S.1:**  $K$ -means clustering for parametric models.

---

**Input:** Observed data  $\{Z_i\}_{i=1}^n$ ; number of clusters  $K$ ; initial cluster centroids  $\{f_j^{(0)}\}_{j=1}^K$ ; loss function  $\rho(z, f)$ ; and maximal iteration  $M$ . Set  $k = 0$ .

**1 Step 1: (Group membership assignment)** For  $i \in [n]$ , set

$$g_i^{(k+1)} = \arg \min_{j \in [K]} \rho(Z_i, f_j^{(k)})$$

**2 Step 2: (Model parameter estimation)** For  $j \in [K]$ , set

$$f_j^{(k+1)} = \arg \min_{f \in \mathbb{R}^d} \sum_{i: g_i^{(k+1)}=j} \rho(Z_i, f).$$

**3 Step 3:** Set  $k = k + 1$  and return to Step 1 until group memberships no longer change or the maximal iteration  $M$  is reached.

**Output:** Scores  $\{\mathbb{S}(Z_i; \mathcal{D}) = g_i^{(k)}\}_{i=1}^n$ .

---

$\rho(\tilde{z}, f) = \|\tilde{z} - f\|_2^2$  to obtain initial labels. Finally, apply Step 2 of Algorithm S.1 with  $\rho(z, f) = (y - x^\top f)^2$  to update centroids, which serve as the required  $\{f_j^{(0)}\}_{j=1}^K$ .

**Remark 3** (On the number of clusters). When the true number of clusters is unknown, we choose  $K$  by minimizing the following Bayesian information criterion:

$$\tilde{K} = \arg \min_{K \in [\bar{K}]} \left\{ \frac{n}{2} \log \left\{ \sum_{j=1}^K \sum_{i: g_i^{(k)}(K)=j} \rho(Z_i, f_j^{(k)}(K)) / n \right\} + K(d+1) \log n \right\},$$

where  $\bar{K}$  is a user-specified upper bound on the number of clusters, and  $g_i^{(k)}(K)$  and  $f_j^{(k)}(K)$  denote the group memberships and parameters, respectively, from the final iteration of Algorithm S.1 when run with  $K$ .

By construction, the output of Algorithm S.1 is invariant to the data order, satisfying Definition 1.

## S.1.2 Deep embedded clustering for high-dimensional data

Deep embedded clustering (Xie et al., 2016) is a modern approach that simultaneously learns a lower-dimensional feature representation and a clustering objective. Let  $g_\theta : \mathcal{Z} \rightarrow \mathbb{R}^s$  (with  $s \ll d$ ) be a nonlinear map, often implemented through deep neural networks, that transforms the data into a low-dimensional latent feature space. The procedure then iteratively refines both the cluster centroids  $\{f_j\}_{j=1}^K$  in the latent space and the parameters  $\theta$ . Algorithm S.2 outlines this procedure.

---

**Algorithm S.2:** Deep embedded clustering for high-dimensional data.

---

**Input:** Observed data  $\{Z_i\}_{i=1}^n$ ; and number of clusters  $K$ .

- 1 **Step 1: (Parameter initialization)** Initial the nonlinear map parameter  $\theta$  and cluster centroids  $\{f_j\}_{j=1}^K$ . See Xie et al. (2016) for details.
- 2 **Step 2: (Joint optimization)** Minimize the KL divergence:

$$\text{KL}(P\|Q) = \sum_{i=1}^n \sum_{j=1}^K p_{ij} \log \frac{p_{ij}}{q_{ij}}$$

via gradient descent, where  $q_{ij}$  is a soft assignment (that measures the probability of assigning sample  $i$  to cluster  $j$ ) between the embedded points  $\{Z'_i = g_\theta(Z_i)\}$  and the cluster centroids  $\{f_j\}_{j=1}^K$ :

$$q_{ij} = \frac{(1 + \|Z'_i - f_j\|_2^2)^{-1}}{\sum_{j'=1}^K (1 + \|Z'_i - f_{j'}\|_2^2)^{-1}},$$

and  $p_{ij}$  is an auxiliary distribution:

$$p_{ij} = \frac{q_{ij}^2 / \sum_{i=1}^n q_{ij}}{\sum_{j'=1}^K \{q_{ij'}^2 / \sum_{i=1}^n q_{ij'}\}}.$$

**Output:** Scores  $\{\mathbb{S}(Z_i; \mathcal{D}) = \arg \max_{j \in [K]} q_{ij}\}_{i=1}^n$ .

---



## S.2 Proofs

### S.2.1 Proof of Theorem 1

**Lemma S.1.** *Let  $W_1, W_2, \dots, W_{B+1}$  be iid random variables. Define*

$$p_B = \frac{\sum_{b=1}^B \mathbb{1}(W_{B+1} < W_b) + U \left\{ 1 + \sum_{b=1}^B \mathbb{1}(W_{B+1} = W_b) \right\}}{B + 1},$$

where  $U \sim \mathcal{U}(0, 1)$  is independent of  $\{W_b\}_{b=1}^{B+1}$ . For any  $\alpha \in (0, 1)$ , it holds that  $\Pr\{p_B < \alpha\} = \alpha$ .

The details of this lemma's proof appear in the proof of Theorem 1 of [Vovk et al. \(2003\)](#). From this lemma, Theorem 1 follows directly.

### S.2.2 Proof of Theorem 2

**Proof of Theorem 2(i):** For any  $i \in \mathcal{I}_\ell$ , we have  $R_{i,\ell} = \sum_{j \in \mathcal{I}_\ell} \mathbb{1}(S_j \leq S_i) = \sum_{j \in \mathcal{I}_\ell} \mathbb{1}(R_j \leq R_i)$ . Then  $(T_{n,1}, T_{n,2}, \dots, T_{n,L})$  can be expressed as a function of  $\{R_i\}_{i=1}^n$ , say

$$(T_{n,1}, T_{n,2}, \dots, T_{n,L}) = \mathbb{G}(R_1, \dots, R_n)$$

for some function  $\mathbb{G} : [n] \rightarrow \mathbb{R}^L$ . Hence, under  $H_0$ ,  $(T_{n,1}, T_{n,2}, \dots, T_{n,L}) \stackrel{d}{=} \mathbb{G}(\pi)$ , where  $\pi \sim \mathcal{U}(\Pi_n)$ . Therefore, the distribution of  $(T_{n,1}, T_{n,2}, \dots, T_{n,L})$  is independent of  $P_1^*$ .

**Proof of Theorem 2(ii):** For notational convenience, denote  $R_i^k = R_{i,(\tau_{k-1}^*, \tau_k^*]}$  for each  $i \in (\tau_{k-1}^*, \tau_k^*]$  and  $k \in [K^* + 1]$ .

**Lemma S.2.** *The sets of ranks  $\{R_i^k : i \in (\tau_{k-1}^*, \tau_k^*]\}$  are mutually independent across  $k \in [K^* + 1]$ . Moreover,  $\tilde{R} = (R_1^1, \dots, R_{\tau_1^*}^1, R_{\tau_1^*+1}^2, \dots, R_{\tau_2^*}^2, \dots, R_{\tau_{K^*+1}^*}^{K^*+1}, \dots, R_{\tau_{K^*+1}^*}^{K^*+1})$  has the same distribution under  $\Pr$  and  $\Pr_{H_0}$ .*

Recall that  $T_{n,\ell} = \mathbb{A}(\{R_{i,\ell}\}_{i \in \mathcal{I}_\ell})$ . Suppose each interval  $\mathcal{I}_\ell$  contains no changepoints. Because  $R_{i,\ell} = \sum_{j \in \mathcal{I}_\ell} \mathbb{1}(S_j \leq S_i) = \sum_{j \in \mathcal{I}_\ell} \mathbb{1}(R_j^k \leq R_i^k)$ ,  $(T_{n,1}, T_{n,2}, \dots, T_{n,L})$  can be written as a function of  $\tilde{R}$ . By Lemma S.2,  $(T_{n,1}, T_{n,2}, \dots, T_{n,L})$  has the same distribution under both  $\Pr$  and  $\Pr_{H_0}$ .

Proof of Lemma S.2: Without loss of generality, assume there is exactly one changepoint in the data. That is, we demonstrate that  $\{R_i^1\}_{i \in (0, \tau_1^*]}$  and  $\{R_i^2\}_{i \in (\tau_1^*, n]}$  are independent, and that  $\tilde{R} = (R_1^1, \dots, R_{\tau_1^*}^1, R_{\tau_1^*+1}^2, \dots, R_n^2)$  has the same distribution under  $\Pr$  and  $\Pr_{H_0}$ . The extension to multiple changepoints is straightforward.

Denote the row vector  $A = (R_1^1, R_2^1, \dots, R_{\tau_1^*}^1)$  and  $B = (R_{\tau_1^*+1}^2, R_2^2, \dots, R_n^2)$ . Let  $\pi_1$  be any permutation of  $\{1, 2, \dots, \tau_1^*\}$  and  $\pi_2$  be any permutation of  $\{1, 2, \dots, n - \tau_1^*\}$ . It suffices to show

$$\Pr\{A = \pi_1, B = \pi_2\} = \Pr\{A = \pi_1\} \Pr\{B = \pi_2\}. \quad (\text{S.1})$$

By the exchangeability of  $S_i$  within each segment, the right-hand side of (S.1) is  $\Pr\{A = \pi_1\} \Pr\{B = \pi_2\} = 1/\{\tau_1^*!(n - \tau_1^*)!\}$ . For the left-hand side of (S.1), without loss of generality, choose  $\pi_1 = (1, 2, 3, 4, \dots, \tau_1^*)$ ,  $\pi_1' = (2, 1, 3, 4, \dots, \tau_1^*)$ , and  $\pi_2 = (1, 2, \dots, n - \tau_1^*)$ . Then we have

$$\begin{aligned} \{A = \pi_1, B = \pi_2\} &= \{S_1 < S_2 < S_3 < S_4 < \dots < S_{\tau_1^*} \text{ and } S_{\tau_1^*+1} < S_{\tau_1^*+2} < \dots < S_n\}, \\ \{A = \pi_1', B = \pi_2\} &= \{S_2 < S_1 < S_3 < S_4 < \dots < S_{\tau_1^*} \text{ and } S_{\tau_1^*+1} < S_{\tau_1^*+2} < \dots < S_n\}. \end{aligned}$$

Because  $(Z_1, Z_2, Z_3, Z_4, \dots, Z_n)$  and  $(Z_2, Z_1, Z_3, Z_4, \dots, Z_n)$  has the same distribution, Definition 1 implies that  $(S_1, S_2, S_3, S_4, \dots, S_n)$  and  $(S_2, S_1, S_3, S_4, \dots, S_n)$  also has the same distribution. Consequently,

$$\Pr\{A = \pi_1, B = \pi_2\} = \Pr\{A = \pi_1', B = \pi_2\}.$$

This shows that for any permutation  $(\pi_1, \pi_2)$ ,  $\Pr\{A = \pi_1, B = \pi_2\}$  is constant. Moreover, since  $\sum_{(\pi_1, \pi_2)} \Pr\{A = \pi_1, B = \pi_2\} = 1$  and there are  $\tau_1^*!(n - \tau_1^*)!$  possible outcomes for  $(\pi_1, \pi_2)$ , it follows that  $\Pr\{A = \pi_1, B = \pi_2\} = 1/\{\tau_1^*!(n - \tau_1^*)!\}$ . Hence, (S.1) is established, confirming the independence of  $A$  and  $B$ .

Because  $A \sim \mathcal{U}(\Pi_{[\tau_1^*]})$  and  $B \sim \mathcal{U}(\Pi_{[n-\tau_1^*]})$  under both  $\Pr$  and  $\Pr_{H_0}$ , and  $A$  and  $B$  are independent, it follows that  $\tilde{R} = (R_1^1, \dots, R_{\tau_1^*}^1, R_{\tau_1^*+1}^2, \dots, R_n^2)$  has the same distribution under  $\Pr$  and  $\Pr_{H_0}$ .

### S.2.3 Proof of Corollary 1

From Theorem 2(i), under  $H_0$ ,  $\max_{\ell \in [L]} T_{n,\ell} \stackrel{d}{=} \|\mathbb{G}(\pi)\|_\infty$ . For  $\pi_1, \dots, \pi_B$  iid from  $\mathcal{U}(\Pi_n)$  and  $\alpha \in (0, 1)$ ,

$$t_{\alpha,B} = \text{the } \lceil (1 - \alpha)(B + 1) \rceil\text{-st smallest value among } \{\|\mathbb{G}(\pi_b)\|_\infty : b \in [B]\}.$$

Then  $\max_{\ell \in [L]} T_{n,\ell} \geq t_{\alpha,B}$  is equivalent to

$$\|\mathbb{G}(\pi)\|_\infty \geq \text{the } \{\lceil (1 - \alpha)(B + 1) \rceil + 1\}\text{-st smallest value among } \{\|\mathbb{G}(\pi)\|_\infty\} \cup \{\|\mathbb{G}(\pi_b)\|_\infty : b \in [B]\}.$$

By exchangeability, the rank of  $\|\mathbb{G}(\pi)\|_\infty$  in that set is uniform on  $\{1, \dots, B + 1\}$ . Thus, under  $H_0$ ,

$$\Pr \left\{ \max_{\ell \in [L]} T_{n,\ell} > t_{\alpha,B} \right\} \leq \frac{(B + 1) - \{\lceil (1 - \alpha)(B + 1) \rceil + 1\}}{B + 1} \leq \alpha.$$

### S.2.4 Proof of Theorem 3

Under  $H_0$ ,  $T_{n,\text{multi}}$  and  $\{\|\mathbb{G}(\pi_b)\|_\infty\}_{b=1}^B$  are iid. By Lemma S.1, the result follows immediately.

### S.2.5 Proof of Proposition 1

Recall that  $d_k = \lceil c_2 \log n / \{Q_k(f_0)\}^2 \rceil + 1$  for  $k \in [K^*]$ , with  $d_0 = d_{K^*+1} = 0$ , and  $h_f(z_1, z_2) = \mathbb{1}(\mathbb{D}(z_2; f) \leq \mathbb{D}(z_1; f)) - 1/2$  for  $f \in \mathcal{F}$ . For  $k \in [K^*]$ , let  $\mathcal{J}_k = (\tau_k^* - d_k, \tau_k^* + d_k]$  and

$$S_{\mathcal{J}_k}(f) = \frac{1}{(2d_k)^{3/2}} \sum_{i=\tau_k^*-d_k+1}^{\tau_k^*} \sum_{j=\tau_k^*+1}^{\tau_k^*+d_k} h_f(Z_i, Z_j).$$

**Lemma S.3.** *Under Assumption 1, there exists some constant  $c_4 > 0$  such that*

$$\Pr \left\{ \max_{1 \leq k \leq K^*} \sup_{f \in \mathcal{F}} |S_{\mathcal{J}_k}(f) - \mathbb{E}[S_{\mathcal{J}_k}(f)]| \leq c_4 \sqrt{\log n} \right\} = 1 + o(1).$$

**Lemma S.4.** *Under Assumption 1, there exist  $c_2 \geq 8(55 + 2c_4 + c_1 c_3)^2$  such that*

$$\Pr \left\{ \min_{1 \leq k \leq K^*} |S_{\mathcal{J}_k}(f_0)| \geq \left( \frac{\sqrt{c_2}}{2\sqrt{2}} - 7 \right) \sqrt{\log n} \right\} \geq 1 - 6/n^3.$$

**Lemma S.5.** *Under  $H_0$ , it holds that*

$$\Pr \left\{ t_{\alpha,B} < 48\sqrt{\log n} \right\} \geq 1 - 6B/n^5.$$

Proof of Proposition 1: Let  $\widehat{\mathcal{R}} = \{\mathcal{I}_{\ell_k} = [s_{\ell_k}, e_{\ell_k}]\}_{k=1}^{\widehat{K}}$ . Define

$$\begin{aligned} A &= \left\{ \|\widehat{f} - f_0\|_{\mathcal{F}} \leq c_1 \sqrt{(\log n)/n} \right\}, \\ B &= \left\{ \max_{1 \leq k \leq K^*} \sup_{f \in \mathcal{F}} |S_{\mathcal{J}_k}(f) - \mathbb{E}[S_{\mathcal{J}_k}(f)]| \leq c_4 \sqrt{\log n} \right\}, \\ C &= \left\{ \min_{1 \leq k \leq K^*} |S_{\mathcal{J}_k}(f_0)| \geq \left( \frac{\sqrt{c_2}}{2\sqrt{2}} - 7 \right) \sqrt{\log n} \right\}, \\ D &= \left\{ t_{\alpha, B} < 48 \sqrt{\log n} \right\}, \\ E &= \left\{ \forall i \in [\widehat{K}], \exists k \in [K^*], \text{ such that } \tau_k^* \notin \mathcal{I}_{\ell_i} \right\}. \end{aligned}$$

By Assumption 1(i), Lemmas S.3–S.5, and Theorem 4, we have

$$\Pr \{A \cap B \cap C \cap D \cap E\} \geq 1 - \Pr \{A^c \cup B^c \cup C^c \cup D^c \cup E^c\} \geq 1 - \alpha + o(1).$$

On  $E$ , each  $\mathcal{I}_{\ell_i}$  contains at least one changepoint. Next, we show each changepoint  $\tau_k^*$  is contained in at least one interval  $\mathcal{I}_{\ell_i}$ . It suffices to verify  $\min_{1 \leq k \leq K^*} |S_{\mathcal{J}_k}(\widehat{f})| > t_{\alpha, B}$ . We have

$$\begin{aligned} & \min_{1 \leq k \leq K^*} |S_{\mathcal{J}_k}(\widehat{f})| \\ & \geq \min_{1 \leq k \leq K^*} |S_{\mathcal{J}_k}(f_0)| - \max_{1 \leq k \leq K^*} |S_{\mathcal{J}_k}(\widehat{f}) - \mathbb{E}[S_{\mathcal{J}_k}(\widehat{f})]| - \max_{1 \leq k \leq K^*} |\mathbb{E}[S_{\mathcal{J}_k}(\widehat{f})] - \mathbb{E}[S_{\mathcal{J}_k}(f_0)]| \\ & \quad - \max_{1 \leq k \leq K^*} |\mathbb{E}[S_{\mathcal{J}_k}(f_0)] - S_{\mathcal{J}_k}(f_0)| \\ & \geq \left( \frac{\sqrt{c_2}}{2\sqrt{2}} - 7 \right) \sqrt{\log n} - c_4 \sqrt{\log n} - c_1 c_3 \sqrt{\log n} - c_4 \sqrt{\log n} \\ & > 48 \sqrt{\log n}, \end{aligned}$$

using Assumption 1(iv) and the fact that  $c_2 \geq 8(55 + 2c_4 + c_1 c_3)^2$ . Event  $D$  then implies that  $\min_{1 \leq k \leq K^*} |S_{\mathcal{J}_k}(\widehat{f})| > t_{\alpha, B}$ . Because Algorithm 1 selects the shortest intervals around each exceedance above  $t_{\alpha, B}$ , each  $\tau_k^*$  must lie within an interval of length no more than  $|\mathcal{J}_k| = 2d_k$ . By Assumption 1(iii) and the recursive nature of ART, no interval contains two or more changepoints, and no changepoint is covered by two or more intervals.

Therefore, on  $A \cap B \cap C \cap D \cap E$ , each  $\mathcal{I}_{\ell_k}$  contains exactly one unique changepoint. This establishes a one-to-one correspondence between  $\{\mathcal{I}_{\ell_k} = [s_{\ell_k}, e_{\ell_k}]\}_{k=1}^{\widehat{K}}$  and  $\{\tau_k^*\}_{k=1}^{K^*}$ , with  $|e_{\ell_k} - s_{\ell_k}| \leq 2d_k$  for each  $k$ . This completes the proof.

## S.2.6 Two-sample U-process theory and proofs of Lemmas S.3–S.5

### S.2.6.1 Two-sample U-process and its properties

We present definitions and properties of two-sample  $U$ -statistics and  $U$ -processes, which will be used to prove Lemmas S.3–S.5. For a comprehensive introduction, see Cléménçon et al. (2021). Let  $X, X_1, \dots, X_n$  and  $Y, Y_1, \dots, Y_m$  be independent iid samples from distributions  $P$  and  $Q$  on measurable spaces  $\mathcal{X}$  and  $\mathcal{Y}$ , respectively.

**Definition 2** (Two-sample  $U$ -statistic/ $U$ -process of degree  $(1, 1)$ ). *Let  $h : \mathcal{X} \times \mathcal{Y} \rightarrow \mathbb{R}$  be square-integrable. The two-sample  $U$ -statistic of degree  $(1, 1)$  with kernel  $h$  is  $U_{n,m}(h) = (nm)^{-1} \sum_{i=1}^n \sum_{j=1}^m h(X_i, Y_j)$ . A class of such  $U$ -statistics indexed by kernels is called a two-sample  $U$ -process.*

The Hájek projection of  $U_{n,m}(h) - \mathbb{E}[U_{n,m}(h)]$  is

$$\widehat{U}_{n,m}(h) = (1/n) \sum_{i=1}^n h_{1,0}(X_i) + (1/m) \sum_{j=1}^m h_{0,1}(Y_j),$$

where  $h_{1,0}(x) = \mathbb{E}_Y[h(x, Y)] - \mathbb{E}[U_{n,m}(h)]$  and  $h_{0,1}(y) = \mathbb{E}_X[h(X, y)] - \mathbb{E}[U_{n,m}(h)]$  for all  $(x, y) \in \mathcal{X} \times \mathcal{Y}$ . The two-sample  $U$ -statistic  $U_{n,m}(h)$  is called *degenerate* if  $h_{1,0}(X)$  and  $h_{0,1}(Y)$  are almost surely zero. Define  $r_{n,m}(h) = U_{n,m}(h) - \mathbb{E}[U_{n,m}(h)] - \widehat{U}_{n,m}(h)$ . Then  $r_{n,m}(h)$  is a degenerate two-sample  $U$ -statistic.

**Lemma S.6** (Lemma 27 in Cléménçon et al. (2021)). *Consider a degenerate two-sample  $U$ -statistic of degree  $(1, 1)$  with a bounded kernel  $h$  such that  $c_h = \sup_{(x,y) \in \mathcal{X} \times \mathcal{Y}} |h(x, y)| < \infty$ . Then for any  $t > 0$ ,  $\Pr\{U_{n,m}(h) \geq t\} \leq \exp\{-nmt^2 / (32c_h^2)\}$ .*

**Definition 3** (VC-class). *A collection  $\mathcal{F}$  of measurable functions on a sample space is called a VC-class with parameters  $a, b > 0$  and constant envelope  $F > 0$  if for any probability measure  $Q$ ,*

$$N(\varepsilon F, \mathcal{F}, L_2(Q)) \leq \left(\frac{a}{\varepsilon}\right)^b,$$

for any  $\varepsilon \in (0, 1)$ , where  $N(\varepsilon, \mathcal{F}, L_2(Q))$  defines the covering number.

By Theorem 2.6.7 in van der Vaart and Wellner (1996), a VC-class of dimension  $\nu < \infty$  with  $F = 1$  corresponds to  $b = 2(\nu - 1)$  and  $a = \{c\nu(16e)^\nu\}^{1/\{2(\nu-1)\}}$ , where  $c$  is a universal constant.

**Lemma S.7** (Lemma 14 in Cléménçon et al. (2021)). Suppose  $\mathcal{F}$  is a VC-class of kernels  $h : \mathcal{X} \times \mathcal{Y} \rightarrow \mathbb{R}$  with parameters  $a, b > 0$  and constant envelope. Then, the sets  $\{h_{1,0}(x) : h \in \mathcal{F}\}$ ,  $\{h_{0,1}(y) : h \in \mathcal{F}\}$ , and  $\{h(x, y) - h_{1,0}(x) - h_{0,1}(y) : h \in \mathcal{F}\}$  are also VC-classes with the same parameters  $a, b$ .

**Lemma S.8** (Lemma 16 in Cléménçon et al. (2021)). Consider a degenerate two-sample  $U$ -process  $\{U_{n,m}(h) : h \in \mathcal{F}\}$  of degree  $(1, 1)$  indexed by asymmetric kernels  $h \in \mathcal{F}$  such that  $\sup_{(x,y) \in \mathcal{X} \times \mathcal{Y}} |h(x, y)| \leq c_h < \infty$  and  $\int_{\mathcal{X} \times \mathcal{Y}} h^2(x, y) dP dQ \leq c_h^2$ . Suppose  $\mathcal{F}$  is a VC-class with parameters  $a, b > 0$  and constant envelope. Then for any  $t > 0$ , there exists a universal constant  $C > 2$  such that

$$\Pr \left\{ \sup_{h \in \mathcal{L}} |U_{n,m}(h)| \geq t \right\} \leq C 2^b (a/c_h)^{2b} \exp \left\{ 4/c_h^2 - nmt^2/(wc_h^2) \right\},$$

for all  $nmt^2 > \max \left\{ 8^4 \log(2) c_h^2 b, (\log(2) c_h^2 b/2)^{1+\zeta} \right\}$  with constants  $\zeta \in (1, 2)$  and  $w = 16^3/2$ .

**Lemma S.9** (Theorem 2.14.9 in van der Vaart and Wellner (1996)). Suppose  $\mathcal{F}$  is a VC-class of measurable functions  $h : \mathcal{X} \rightarrow [0, 1]$  with parameters  $a, b > 0$  and constant envelope. Then for any  $t > 0$ ,

$$\Pr \left\{ \sup_{h \in \mathcal{F}} \sqrt{n} \left| \frac{1}{n} \sum_{i=1}^n h(X_i) - \mathbb{E}[h(X)] \right| > t \right\} \leq \left( \frac{ct}{\sqrt{b}} \right)^b \exp \{-2t^2\},$$

where the constant  $c$  depends only on  $a$ .

### S.2.6.2 Proof of Lemma S.3

Recall that

$$S_{\mathcal{J}_k}(f) = \frac{1}{(2d_k)^{3/2}} \sum_{i=\tau_k^*-d_k+1}^{\tau_k^*} \sum_{j=\tau_k^*+1}^{\tau_k^*+d_k} h_f(Z_i, Z_j) = \frac{\sqrt{d_k}}{2\sqrt{2}} U_{d_k, d_k}(h_f),$$

where  $h_f(Z_i, Z_j) = \mathbb{1}(\mathbb{D}(Z_j; f) \leq \mathbb{D}(Z_i; f)) - 1/2$ , with  $Z_i \sim P_k^*$  and  $Z_j \sim P_{k+1}^*$ . The Hájek projection of  $U_{d_k, d_k}(h_f)$  is given by

$$\widehat{U}_{d_k, d_k}(h_f) = (1/d_k) \sum_{i=\tau_k^*-d_k+1}^{\tau_k^*} h_{f,1,0}(Z_i) + (1/d_k) \sum_{j=\tau_k^*+1}^{\tau_k^*+d_k} h_{f,0,1}(Z_j),$$

where  $h_{f,1,0}(z_i) = \mathbb{E}_{Z_{\tau_k^*+1}} [h_f(z_i, Z_{\tau_k^*+1})] - \mathbb{E}[U_{d_k, d_k}(h_f)]$  and  $h_{f,0,1}(z_j) = \mathbb{E}_{Z_{\tau_k^*}} [h_f(Z_{\tau_k^*}, z_j)] - \mathbb{E}[U_{d_k, d_k}(h_f)]$ . By Assumption 1(ii),  $\{h_f : f \in \mathcal{F}\}$  is a VC-class with parameters  $a = \{c\nu(16e)^\nu\}^{1/\{2(\nu-1)\}}$ ,  $b = 2(\nu-1)$ , and constant envelope 1.

Denote  $r_{d_k, d_k}(h_f) = U_{d_k, d_k}(h_f) - \mathbb{E}[U_{d_k, d_k}(h_f)] - \widehat{U}_{d_k, d_k}(h_f)$ , then

$$\begin{aligned} r_{d_k, d_k}(h_f) &= \frac{1}{d_k^2} \sum_{i=\tau_k^*-d_k+1}^{\tau_k^*} \sum_{j=\tau_k^*+1}^{\tau_k^*+d_k} h_f(Z_i, Z_j) - \mathbb{E}[h_f(Z_i, Z_j)] - h_{f,1,0}(Z_i) - h_{f,0,1}(Z_j) \\ &= \frac{1}{d_k^2} \sum_{i=\tau_k^*-d_k+1}^{\tau_k^*} \sum_{j=\tau_k^*+1}^{\tau_k^*+d_k} h'_f(Z_i, Z_j), \end{aligned}$$

where  $h'_f(Z_i, Z_j) = h_f(Z_i, Z_j) - \mathbb{E}[h_f(Z_i, Z_j)] - h_{f,1,0}(Z_i) - h_{f,0,1}(Z_j)$ . Notice that  $\{r_{d_k, d_k}(h_f) : f \in \mathcal{F}\}$  is a degenerate two-sample  $U$ -process. By Lemma S.7,  $\{h'_f : f \in \mathcal{F}\}$  is a VC-class with parameter  $(a, b)$ . Noticing that  $|h'_f(Z_i, Z_j)| \leq 3$ , Lemma S.8 implies that

$$\begin{aligned} \Pr \left\{ \sup_{f \in \mathcal{F}} \left| U_{d_k, d_k}(h_f) - \mathbb{E}[U_{d_k, d_k}(h_f)] - \widehat{U}_{d_k, d_k}(h_f) \right| \geq x \right\} \\ \leq C2^b (a/c_h)^{2b} \exp \{4/c_h^2 - d_k^2 x^2 / (wc_h^2)\}, \end{aligned}$$

for all  $d_k^2 x^2 > \max \{8^4 \log(2)c_h^2 b, (\log(2)c_h^2 b/2)^{1+\zeta}\}$ . Hence,

$$\begin{aligned} \Pr \left\{ \sup_{f \in \mathcal{F}} \left| S_{\mathcal{J}_k}(f) - \mathbb{E}[S_{\mathcal{J}_k}(f)] - \frac{\sqrt{d_k}}{2\sqrt{2}} \widehat{U}_{d_k, d_k}(h_f) \right| \geq x \right\} \\ \leq C2^b (a/c_h)^{2b} \exp \{4/c_h^2 - 8d_k x^2 / (wc_h^2)\}, \end{aligned}$$

for all  $8d_k x^2 > \max \{8^4 \log(2)c_h^2 b, (\log(2)c_h^2 b/2)^{1+\zeta}\}$ .

Next, consider the Hájek projection  $\widehat{U}_{d_k, d_k}(h_f)$ . Direct calculation shows  $|h_{f,1,0}(Z_i)| \leq 1$ ,  $|h_{f,0,1}(Z_j)| \leq 1$ ,  $\mathbb{E}[h_{f,1,0}(Z_i)] = 0$ , and  $\mathbb{E}[h_{f,0,1}(Z_j)] = 0$ . By Lemma S.7, both  $\{h_{f,1,0} : f \in \mathcal{F}\}$  and  $\{h_{f,0,1} : f \in \mathcal{F}\}$  are VC-classes with parameter  $(a, b)$ . Applying Lemma S.9, we have

$$\begin{aligned} \Pr \left\{ \sup_{f \in \mathcal{F}} \sqrt{d_k} \left| \frac{1}{d_k} \sum_{i=\tau_k^*-d_k+1}^{\tau_k^*} h_{f,1,0}(Z_i) \right| \geq x \right\} &\leq \left( \frac{cx}{\sqrt{b}} \right)^b \exp \{-2x^2\}, \\ \Pr \left\{ \sup_{f \in \mathcal{F}} \sqrt{d_k} \left| \frac{1}{d_k} \sum_{j=\tau_k^*+1}^{\tau_k^*+d_k} h_{f,0,1}(Z_j) \right| \geq x \right\} &\leq \left( \frac{cx}{\sqrt{b}} \right)^b \exp \{-2x^2\}. \end{aligned}$$

This further implies that

$$\Pr \left\{ \sup_{f \in \mathcal{F}} \left| \frac{\sqrt{d_k}}{2\sqrt{2}} \widehat{U}_{d_k, d_k}(h_{f_0}) \right| \geq x \right\} \leq 2 \left( \frac{cx}{\sqrt{b}} \right)^b \exp \{-4x^2\}.$$

By the triangle inequality,

$$\begin{aligned}
& \Pr \left\{ \max_{1 \leq k \leq K^*} \sup_{f \in \mathcal{F}} |S_{\mathcal{J}_k}(f) - \mathbb{E}[S_{\mathcal{J}_k}(f)]| \geq 2x \right\} \\
& \leq \Pr \left\{ \max_{1 \leq k \leq K^*} \sup_{f \in \mathcal{F}} \left| S_{\mathcal{J}_k}(f) - \mathbb{E}[S_{\mathcal{J}_k}(f)] - \frac{\sqrt{d_k}}{2\sqrt{2}} \widehat{U}_{d_k, d_k}(h_f) \right| \geq x \right\} \\
& \quad + \Pr \left\{ \max_{1 \leq k \leq K^*} \sup_{f \in \mathcal{F}} \left| \frac{\sqrt{d_k}}{2\sqrt{2}} \widehat{U}_{d_k, d_k}(h_f) \right| \geq x \right\} \\
& \leq K^* C 2^b (a/c_h)^{2b} \exp \{4/c_h^2 - 8d_k x^2 / (w c_h^2)\} + 2K^* \left( cx/\sqrt{b} \right)^b \exp \{-4x^2\}.
\end{aligned}$$

Setting  $2x = c_4 \sqrt{\log n}$  finishes the argument, showing that

$$\Pr \left\{ \max_{1 \leq k \leq K^*} \sup_{f \in \mathcal{F}} |S_{\mathcal{J}_k}(f) - \mathbb{E}[S_{\mathcal{J}_k}(f)]| < c_4 \sqrt{\log n} \right\} = 1 + o(1)$$

for some constant  $c_4 > 0$ .

### S.2.6.3 Proof of Lemma S.4

Arguing as in the proof of Lemma S.3 but applying Lemma S.6, we get

$$\Pr \left\{ \left| U_{d_k, d_k}(h_{f_0}) - \mathbb{E}[U_{d_k, d_k}(h_{f_0})] - \widehat{U}_{d_k, d_k}(h_{f_0}) \right| \geq x \right\} \leq 2 \exp \{-d_k^2 x^2 / 72\},$$

which implies

$$\Pr \left\{ \left| S_{\mathcal{J}_k}(f_0) - \frac{\sqrt{d_k}}{2\sqrt{2}} \mathbb{E}[U_{d_k, d_k}(h_{f_0})] - \frac{\sqrt{d_k}}{2\sqrt{2}} \widehat{U}_{d_k, d_k}(h_{f_0}) \right| \geq x \right\} \leq 2 \exp \{-d_k x^2 / 9\}.$$

Consider the Hájek projection

$$\widehat{U}_{d_k, d_k}(h_{f_0}) = (1/d_k) \sum_{i=\tau_k^*-d_k+1}^{\tau_k^*} h_{f_0, 1, 0}(Z_i) + (1/d_k) \sum_{j=\tau_k^*+1}^{\tau_k^*+d_k} h_{f_0, 0, 1}(Z_j).$$

By Hoeffding's inequality,

$$\begin{aligned}
& \Pr \left\{ \left| \frac{1}{d_k} \sum_{i=\tau_k^*-d_k+1}^{\tau_k^*} h_{f_0, 1, 0}(Z_i) \right| \geq x \right\} \leq 2 \exp \{-2d_k x^2\}, \\
& \Pr \left\{ \left| \frac{1}{d_k} \sum_{j=\tau_k^*+1}^{\tau_k^*+d_k} h_{f_0, 0, 1}(Z_j) \right| \geq x \right\} \leq 2 \exp \{-2d_k x^2\}.
\end{aligned}$$



Thus,

$$\Pr \left\{ \left| \frac{\sqrt{d_k}}{2\sqrt{2}} \widehat{U}_{d_k, d_k}(h_{f_0}) \right| \geq x \right\} \leq 4 \exp \{-4x^2\}.$$

By the triangle inequality,

$$\begin{aligned} \Pr \left\{ \left| S_{\mathcal{J}_k}(f_0) \right| < \left| \frac{\sqrt{d_k}}{2\sqrt{2}} \mathbb{E} \left[ U_{d_k, d_k}(h_{f_0}) \right] \right| - \sqrt{\log n} - \frac{6\sqrt{\log n}}{\sqrt{d_k}} \right\} \\ \leq \Pr \left\{ \left| S_{\mathcal{J}_k}(f_0) - \frac{\sqrt{d_k}}{2\sqrt{2}} \mathbb{E} \left[ U_{d_k, d_k}(h_{f_0}) \right] \right| \geq \sqrt{\log n} + \frac{6\sqrt{\log n}}{\sqrt{d_k}} \right\} \\ \leq \Pr \left\{ \left| S_{\mathcal{J}_k}(f_0) - \frac{\sqrt{d_k}}{2\sqrt{2}} \mathbb{E} \left[ U_{d_k, d_k}(h_{f_0}) \right] - \frac{\sqrt{d_k}}{2\sqrt{2}} \widehat{U}_{d_k, d_k}(h_{f_0}) \right| \geq \frac{6\sqrt{\log n}}{\sqrt{d_k}} \right\} \\ \quad + \Pr \left\{ \left| \frac{\sqrt{d_k}}{2\sqrt{2}} \widehat{U}_{d_k, d_k}(h_{f_0}) \right| \geq \sqrt{\log n} \right\} \\ \leq 2 \exp(-4 \log n) + 4 \exp(-4 \log n) = 6/n^4. \end{aligned}$$

Note that  $\mathbb{E} [U_{d_k, d_k}(h_{f_0})] = Q_k(f_0)$ . By definition  $d_k = \lceil c_2 \log n / \{Q_k(f_0)\}^2 \rceil + 1$ , we have

$$\left| \frac{\sqrt{d_k}}{2\sqrt{2}} \mathbb{E} [U_{d_k, d_k}(h_{f_0})] \right| > \frac{\sqrt{c_2}}{2\sqrt{2}} \sqrt{\log n},$$

implying

$$\Pr \left\{ |S_{\mathcal{J}_k}(f_0)| \geq \left( \frac{\sqrt{c_2}}{2\sqrt{2}} - 7 \right) \sqrt{\log n} \right\} \geq 1 - 6/n^4.$$

A union bound then gives

$$\begin{aligned} \Pr \left\{ \min_{1 \leq k \leq K^*} |S_{\mathcal{J}_k}(f_0)| \geq \left( \frac{\sqrt{c_2}}{2\sqrt{2}} - 7 \right) \sqrt{\log n} \right\} \\ \geq 1 - \Pr \left\{ \exists k \in [K^*] \text{ such that } |S_{\mathcal{J}_k}(f_0)| < \left( \frac{\sqrt{c_2}}{2\sqrt{2}} - 7 \right) \sqrt{\log n} \right\} \\ \geq 1 - 6/n^3. \end{aligned}$$

#### S.2.6.4 Proof of Lemma S.5

Recall that under  $H_0$ ,  $\max_{\ell \in [L]} T_{n, \ell} \stackrel{d}{=} \|\mathbb{G}(\pi)\|_\infty$ , and

$t_{\alpha, B}$  = the  $\lceil (1 - \alpha)(B + 1) \rceil$ -st smallest value among  $\{\|\mathbb{G}(\pi_b)\|_\infty : b \in [B]\}$ ,

where for any  $\mathcal{I}_\ell = [s_\ell, e_\ell]$ ,

$$T_{n,\ell} = \sup_{t \in [s_\ell, e_\ell]} \left| \frac{1}{(e_\ell - s_\ell)^{3/2}} \sum_{i=s_\ell}^t \sum_{j=t+1}^{e_\ell} \left( \mathbb{1}(S_j \leq S_i) - \frac{1}{2} \right) \right|.$$

The proof strategy is to characterize the tail probability of  $T_{n,\ell}$ . Although  $(S_1, S_2, \dots, S_n)$  is exchangeable under  $\Pr_{H_0}$ ,  $T_{n,\ell}$  is not a two-sample  $U$ -statistic. However, treating  $S_1, S_2, \dots, S_n$  as iid continuous random variables leaves the distribution of  $T_{n,\ell}$  unchanged. Hence, in the following we assume  $S_1, S_2, \dots, S_n$  are iid continuous random variables.

For notational convenience, define

$$S(s_\ell, t, e_\ell) = \frac{1}{(e_\ell - s_\ell)^{3/2}} \sum_{i=s_\ell}^t \sum_{j=t+1}^{e_\ell} h(S_i, S_j),$$

$$U(s_\ell, t, e_\ell) = \frac{1}{(t - s_\ell + 1)(e_\ell - t)} \sum_{i=s_\ell}^t \sum_{j=t+1}^{e_\ell} h(S_i, S_j),$$

where  $h(S_i, S_j) = \mathbb{1}(S_j \leq S_i) - 1/2$ . Because  $\mathbb{E}[U(s_\ell, t, e_\ell)] = 0$ , applying Lemma S.6 yields

$$\Pr_{H_0} \left\{ \left| U(s_\ell, t, e_\ell) - \widehat{U}(s_\ell, t, e_\ell) \right| \geq x \right\} \leq 2 \exp \left\{ -(t - s_\ell + 1)(e_\ell - t)x^2/72 \right\},$$

where  $\widehat{U}(s_\ell, t, e_\ell) = (1/(t - s_\ell + 1)) \sum_{i=s_\ell}^t h_{1,0}(S_i) + (1/(e_\ell - t)) \sum_{j=t+1}^{e_\ell} h_{0,1}(S_j)$  is the Hájek projection of  $U(s_\ell, t, e_\ell)$ . It follows that

$$\Pr_{H_0} \left\{ \left| S(s_\ell, t, e_\ell) - \frac{(t - s_\ell + 1)(e_\ell - t)}{(e_\ell - s_\ell)^{3/2}} \widehat{U}(s_\ell, t, e_\ell) \right| \geq x \right\} \leq 2 \exp \left\{ -x^2/72 \right\}.$$

Consider the Hájek projection  $\widehat{U}(s_\ell, t, e_\ell)$  and applying Hoeffding's inequality in a manner similar to Lemma S.4, we obtain

$$\Pr_{H_0} \left\{ \left| \frac{1}{t - s_\ell + 1} \sum_{i=s_\ell}^t h_{1,0}(Z_i) \right| \geq x \right\} \leq 2 \exp \left\{ -2(t - s_\ell + 1)x^2 \right\},$$

$$\Pr_{H_0} \left\{ \left| \frac{1}{e_\ell - t} \sum_{j=t+1}^{e_\ell} h_{0,1}(Z_j) \right| \geq x \right\} \leq 2 \exp \left\{ -2(e_\ell - t)x^2 \right\}.$$

Hence,

$$\Pr_{H_0} \left\{ \frac{(t - s_\ell + 1)(e_\ell - t)}{(e_\ell - s_\ell)^{3/2}} \left| \frac{1}{t - s_\ell + 1} \sum_{i=s_\ell}^t h_{1,0}(Z_i) \right| \geq x \right\} \leq 2 \exp \left\{ -x^2 \right\},$$

$$\Pr_{H_0} \left\{ \left| \frac{(t - s_\ell + 1)(e_\ell - t)}{(e_\ell - s_\ell)^{3/2}} \left| \frac{1}{e_\ell - t} \sum_{j=t+1}^{e_\ell} h_{0,1}(Z_j) \right| \right| \geq x \right\} \leq 2 \exp \{-x^2\}.$$

A triangle inequality gives

$$\Pr_{H_0} \left\{ \left| \frac{(t - s_\ell + 1)(e_\ell - t)}{(e_\ell - s_\ell)^{3/2}} \widehat{U}(s_\ell, t, e_\ell) \right| \geq x \right\} \leq 4 \exp \{-x^2/4\}.$$

Combining these results,

$$\begin{aligned} & \Pr_{H_0} \{ |S(s_\ell, t, e_\ell)| \geq 2x \} \\ & \leq \Pr_{H_0} \left\{ \left| S(s_\ell, t, e_\ell) - \frac{(t - s_\ell + 1)(e_\ell - t)}{(e_\ell - s_\ell)^{3/2}} \widehat{U}(s_\ell, t, e_\ell) \right| \geq x \right\} \\ & \quad + \Pr_{H_0} \left\{ \left| \frac{(t - s_\ell + 1)(e_\ell - t)}{(e_\ell - s_\ell)^{3/2}} \widehat{U}(s_\ell, t, e_\ell) \right| \geq x \right\} \\ & \leq 4 \exp \{-x^2/4\} + 2 \exp \{-x^2/72\} \leq 6 \exp \{-x^2/72\}. \end{aligned}$$

By a union bound,

$$\Pr_{H_0} \left\{ \max_{\ell \in [L]} T_{n,\ell} > 2x \right\} \leq n^3 \max_{(s_\ell, t, e_\ell)} \Pr \{ |S(s_\ell, t, e_\ell)| \geq 2x \} \leq 6n^3 \exp \{-x^2/72\}.$$

It follows that

$$\Pr_{H_0} \left\{ \max_{b \in [B]} \|\mathbb{G}(\pi_b)\|_\infty > 2x \right\} \leq 6Bn^3 \exp \{-x^2/72\},$$

Taking  $x = 24\sqrt{\log n}$  yields

$$\Pr_{H_0} \left\{ \max_{b \in [B]} \|\mathbb{G}(\pi_b)\|_\infty > 48\sqrt{\log n} \right\} \leq 6B/n^5,$$

thus  $t_{\alpha,B} < 48\sqrt{\log n}$  with probability at least  $1 - 6B/n^5$ .

### S.3 Additional simulation results

Table S.1 summaries the ART methodology and its corresponding applications in numerical experiments presented in the supplementary material.

Table S.1: Summary of the ART methodology.

Models	Transformation	Aggregation	Result
Mean	$K$ -means	Rank CUSUM	Figure S.1, Figure S.2
	$\mathbb{D}(z; \hat{f}_{\mathcal{D}}) = -\phi(z - \hat{\theta}_{\mathcal{D}})$	Nonparametric likelihood	Figure S.2
Regression	$K$ -means	Rank CUSUM	Table S.2, Table S.3, Table S.4
	$\mathbb{D}(z; \hat{f}_{\mathcal{D}}) = (y - x^{\top} \hat{\theta}_{\mathcal{D}})^2$	Nonparametric likelihood	Table S.2, Table S.3
Distribution	$K$ -means	Rank CUSUM	Figure S.2
	$\mathbb{D}(z; \hat{f}_{\mathcal{D}}) = -\phi(z)$	Nonparametric likelihood	Figure S.2

### S.3.1 The impact of parameter $B$

In this section, we examine the performance of the ART test under different choices of  $B$ . We focus on AMOC scenarios in the mean change model to illustrate how  $B$  affects size and power; analogous findings hold for other models. The model setup and implementation of ART follows exactly the procedures described in Section 4.1.1.

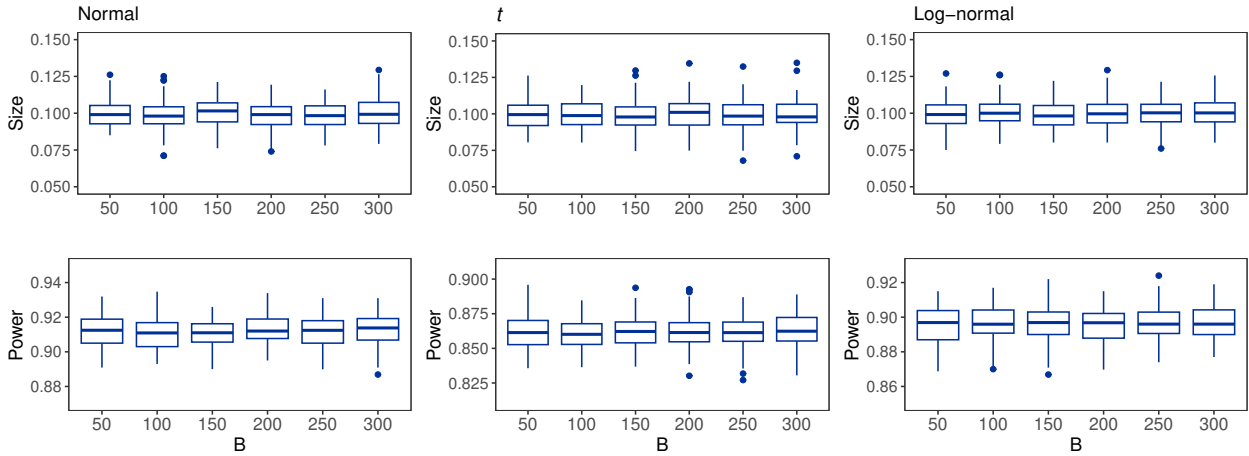


Figure S.1: Empirical size and power comparisons for varying  $B$  under various error distributions, with  $\alpha = 0.1$  and  $(n, d, c_{\theta}) = (200, 100, 0.4)$ .

Figure S.1 presents boxplots of empirical size and power under various error distributions, based on 100 runs each with 1,000 replications. The results show that the test size is very stable across different values of  $B$ , consistent with our theoretical findings. The power remains largely robust, with slight improvements observed for larger values of  $B$ .

### S.3.2 Deviance versus clustering transformations

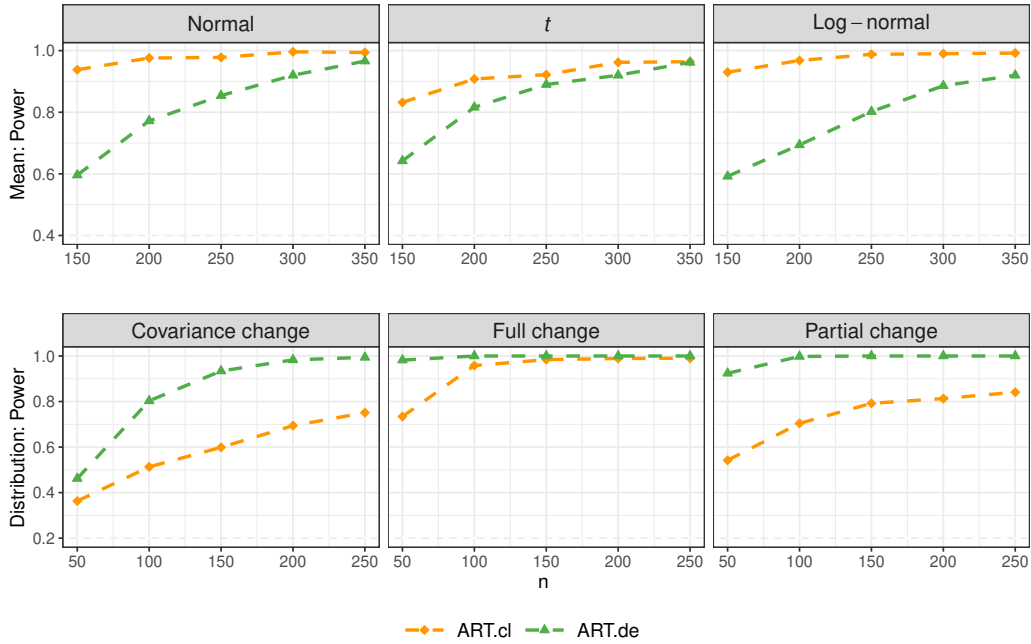


Figure S.2: Empirical power of the clustering-based (ART.cl) and deviance-based (ART.de) ART tests under mean and distributional change models.

In the ART method, any symmetric transformation ensures exact control of the test size. However, the test power depends on the choice of transformation. Below, we compare the deviance and clustering transformations proposed in Section 2.2.

We first examine mean changes and distributional changes. The top row of Figure S.2 compares power across deviance and clustering transformations while varying  $n$  under mean change models. Data are generated as in Section 4.1.1 with  $d = 5$ ,  $s = 3$ ,  $\mathcal{T}^* = \{\lfloor 0.3n \rfloor\}$ , and  $c_P = (0.25, \sqrt{3}, 1)$  and  $c_\theta = (0.5, 0.8, 0.1)$  for normal,  $t$ , and log-normal errors, respectively.

The second row of Figure S.2 illustrates power under distributional changes, investigating three scenarios: (i) Covariance change:  $P_1^* = \mathcal{N}(0, I/2)$  and  $P_2^* = \mathcal{N}(\mu_1, (0.9^{|i-j|}))$  with  $\mu_1 = (0.6, -0.6, 0.6, 0_{d-3}^\top)^\top$ ; (ii) Full change:  $P_1^* = \mathcal{N}(\mu_1, I)$  and  $P_2^* = \{t(3)\}^d$ ; and (iii) Partial change:  $P_1^* = \mathcal{N}(\mu_1, I)$  and  $P_2^* = \{t(3)\}^s \cdot \{\mathcal{N}(0, 1)\}^{d-s}$ , where  $s = \lfloor 0.6d \rfloor$ . We set  $d = 5$  and  $\mathcal{T}^* = \{\lfloor 0.3n \rfloor\}$ .

Next, we consider changes in regression coefficients under two scenarios:

Table S.2: Empirical size and power of the clustering-based (ART.cl) and deviance-based (ART.de) ART tests under various error distributions for the regression model scenario (i).

$\tau_1^*$	Error	$(n, d)$	Null		Small change		Large change	
			ART.cl	ART.de	ART.cl	ART.de	ART.cl	ART.de
[0.3n]	Normal	(100,200)	0.097	0.102	0.640	0.566	0.791	0.875
		(200,200)	0.092	0.113	0.799	0.829	0.906	0.997
		(400,200)	0.095	0.098	0.863	0.987	0.922	1.000
	$t$	(100,200)	0.102	0.096	0.387	0.368	0.549	0.656
		(200,200)	0.089	0.101	0.624	0.635	0.805	0.944
		(400,200)	0.092	0.088	0.715	0.901	0.866	1.000
	Log-normal	(100,200)	0.106	0.095	0.378	0.337	0.559	0.629
		(200,200)	0.111	0.091	0.574	0.585	0.787	0.914
		(400,200)	0.099	0.098	0.693	0.862	0.864	1.000
[0.4n]	Normal	(100,200)	0.098	0.093	0.656	0.716	0.765	0.962
		(200,200)	0.095	0.098	0.791	0.916	0.877	0.999
		(400,200)	0.096	0.105	0.893	0.999	0.899	1.000
	$t$	(100,200)	0.100	0.101	0.423	0.509	0.580	0.818
		(200,200)	0.087	0.102	0.625	0.773	0.795	0.985
		(400,200)	0.115	0.099	0.759	0.971	0.874	1.000
	Log-normal	(100,200)	0.095	0.094	0.418	0.466	0.588	0.820
		(200,200)	0.097	0.094	0.607	0.692	0.778	0.983
		(400,200)	0.093	0.104	0.752	0.933	0.876	1.000
[0.5n]	Normal	(100,200)	0.093	0.099	0.642	0.751	0.748	0.960
		(200,200)	0.106	0.105	0.823	0.956	0.878	1.000
		(400,200)	0.100	0.115	0.922	1.000	0.911	1.000
	$t$	(100,200)	0.098	0.101	0.399	0.579	0.575	0.878
		(200,200)	0.097	0.108	0.622	0.829	0.758	0.993
		(400,200)	0.103	0.099	0.789	0.989	0.870	1.000
	Log-normal	(100,200)	0.089	0.103	0.388	0.506	0.608	0.858
		(200,200)	0.106	0.101	0.610	0.805	0.772	0.988
		(400,200)	0.097	0.098	0.812	0.961	0.874	1.000

Table S.3: Empirical size and power of the clustering-based (ART.cl) and deviance-based (ART.de) ART tests under various error distributions for the regression model scenario (ii).

$\tau_1^*$	Error	$(n, d)$	Null		Small change		Large change	
			ART.cl	ART.de	ART.cl	ART.de	ART.cl	ART.de
[0.3n]	Normal	(100,200)	0.103	0.103	0.714	0.226	0.729	0.541
		(200,200)	0.094	0.097	0.856	0.379	0.878	0.825
		(400,200)	0.114	0.092	0.848	0.595	0.975	0.991
	$t$	(100,200)	0.099	0.101	0.450	0.186	0.520	0.335
		(200,200)	0.108	0.092	0.738	0.264	0.798	0.644
		(400,200)	0.098	0.109	0.914	0.427	0.933	0.921
	Log-normal	(100,200)	0.107	0.096	0.410	0.162	0.497	0.361
		(200,200)	0.108	0.099	0.684	0.256	0.789	0.619
		(400,200)	0.089	0.092	0.852	0.417	0.884	0.887
[0.4n]	Normal	(100,200)	0.101	0.097	0.763	0.297	0.766	0.730
		(200,200)	0.089	0.098	0.876	0.484	0.922	0.952
		(400,200)	0.097	0.111	0.923	0.782	0.977	1.000
	$t$	(100,200)	0.099	0.101	0.518	0.237	0.571	0.579
		(200,200)	0.108	0.110	0.812	0.382	0.829	0.852
		(400,200)	0.107	0.101	0.946	0.575	0.959	0.988
	Log-normal	(100,200)	0.097	0.100	0.511	0.226	0.596	0.501
		(200,200)	0.086	0.092	0.833	0.363	0.850	0.814
		(400,200)	0.089	0.099	0.922	0.569	0.931	0.980
[0.5n]	Normal	(100,200)	0.110	0.108	0.730	0.337	0.803	0.772
		(200,200)	0.096	0.107	0.916	0.555	0.941	0.964
		(400,200)	0.101	0.098	0.979	0.832	0.989	0.999
	$t$	(100,200)	0.103	0.099	0.505	0.279	0.623	0.660
		(200,200)	0.091	0.108	0.844	0.474	0.906	0.890
		(400,200)	0.097	0.099	0.965	0.676	0.966	0.995
	Log-normal	(100,200)	0.104	0.097	0.508	0.236	0.601	0.636
		(200,200)	0.094	0.103	0.804	0.396	0.902	0.868
		(400,200)	0.099	0.094	0.968	0.629	0.982	0.991

- (i)  $\theta_1^* = (0.5, 0, -0.5, 0_{d-3}^\top)^\top$  and  $\theta_2^* = \theta_1^* + c_\theta \cdot D_{1,s}$  with  $D_{1,s} = (-1, 1, -1, 1, -1, 0_{d-5}^\top)^\top$ ;
- (ii)  $\theta_1^* = (0.5, -0.5, -0.5, 0.5, 0_{d-4}^\top)^\top$  and  $\theta_2^* = \theta_1^* + c_\theta \cdot D_{1,s}$ .

We use the same three error distributions as in Section 4.1.1. Tables S.2–S.3 display empirical size and power for  $\tau_1^* = \{\lfloor 0.3n \rfloor, \lfloor 0.4n \rfloor, \lfloor 0.5n \rfloor\}$  and  $c_\theta = \{0.5, 0.7\}$  corresponding to small and large changes.

Both clustering and deviance transformations exhibit satisfactory performance, with power increasing as sample size or the magnitude of change grows. Clustering transformations can incorporate diverse clustering algorithms, making them adaptable to complex data. Meanwhile, deviance transformations are computationally efficient and straightforward to implement. Both approaches each have their own merits, rendering them reliable options for a wide range of practical applications.

### S.3.3 Departures from independence

We assess ART when the data  $\{Z_i\}_{i=1}^n$  are not independent. Specifically, we consider regression models with an autoregressive (AR) process among  $\{\varepsilon_i\}_{i=1}^n$ :  $\varepsilon_i = 0.6\varepsilon_{i-1} + \sqrt{1 - 0.6^2}e_i$ , where  $e_i$  follows one of the three error distributions  $P_{\varepsilon,1}$  described in Section 4.1. The model settings aligns with those in Section 4.1, focusing on changes in regression coefficients for both small and large shifts ( $c_\theta = 0.5$  and  $c_\theta = 1$ ).

Table S.4 compares the performance of ART under independent and such AR(1) dependent scenarios, with  $\alpha = 0.1$ . The empirical size remains near the nominal level in both cases, while the power under the AR(1) setting is comparable to that under independence. These outcomes highlight the robustness and effectiveness of ART for certain nonexchangeable data structures, meriting further theoretical investigation.



Table S.4: Empirical size and power of ART under independent and AR(1) error structures for various error distributions in regression models.

Error	$(n, d)$	Null		Small change		Large change	
		Independent	AR(1)	Independent	AR(1)	Independent	AR(1)
Normal	(50,100)	0.096	0.110	0.401	0.402	0.445	0.443
	(100,100)	0.101	0.104	0.581	0.594	0.765	0.761
	(200,100)	0.091	0.111	0.621	0.654	0.946	0.941
	(50,200)	0.102	0.107	0.259	0.284	0.285	0.334
	(100,200)	0.108	0.112	0.458	0.490	0.753	0.733
	(200,200)	0.097	0.105	0.601	0.571	0.916	0.932
$t$	(50,100)	0.094	0.110	0.301	0.299	0.362	0.335
	(100,100)	0.106	0.114	0.405	0.403	0.645	0.636
	(200,100)	0.099	0.106	0.463	0.438	0.902	0.901
	(50,200)	0.097	0.106	0.205	0.194	0.259	0.245
	(100,200)	0.092	0.120	0.293	0.356	0.613	0.616
	(200,200)	0.093	0.123	0.368	0.394	0.899	0.879
Log-normal	(50,100)	0.104	0.112	0.231	0.209	0.309	0.314
	(100,100)	0.101	0.105	0.382	0.345	0.619	0.618
	(200,100)	0.105	0.098	0.395	0.404	0.896	0.896
	(50,200)	0.098	0.104	0.187	0.159	0.218	0.236
	(100,200)	0.094	0.113	0.278	0.282	0.593	0.611
	(200,200)	0.105	0.112	0.329	0.352	0.876	0.880